Energy Advances

ROYAL SOCIETY OF CHEMISTRY

REVIEW ARTICLE

View Article Online
View Journal | View Issue

Cite this: *Energy Adv.*, 2022, 1, 738

Transition metal quantum dots for the electrocatalytic hydrogen evolution reaction: recent progresses and challenges

Brahmari Honnappa,[a] Sathya Mohan,[b] Mariyappan Shanmugam,[b] Ashil Augustin,[b] Prince J. J. Sagayaraj,[b] Chitiphon Chuaicham,[c] Saravanan Rajendran,[d] Tuan K. A. Hoang,[e] Keiko Sasaki[c] and Karthikeyan Sekar*[b]

Hydrogen, a renewable, green, clean, and energy source since long, has been attracting the interest of many researchers as hydrogen is produced alongside oxygen *via* water splitting using a simple electrochemical method. To realizehydrogen economy, sustainable hydrogen generation is a major expedient. Several reports have surfaced on water splitting using various catalysts with simultaneous hydrogen and oxygen evolution, among which transition metal quantum dots (TMQDs) are intriguingly great candidates for industrialization due to their extraordinary properties such as optical, electrical, and fluorescence. This study summarizes in-depth the basic concepts of the hydrogen evolution reaction and reviews the most recent advances in TMQDs as electrocatalysts, where a deeper evaluation of the synthesis, characteristics, and properties of TMQDs as well as insights into the catalyst's activity, morphology, composition, and other factors, are correlatively addressed. There are well-developed strategies to date for effectively modifying the activity and increasing the active sites, among which, quantum confinement is studied and emphasized. The prospects and difficulties in electrochemical water splitting are then analysed.

Received 15th July 2022,
Accepted 28th September 2022

DOI: 10.1039/d2ya00181k

rsc.li/energy-advances

[a] *Department of Physics and Nanotechnology, SRM Institute of Science and Technology, Kattankulathur, Tamil Nadu 603203, India*
[b] *Sustainable Energy and Environmental Research Laboratory, Department of Chemistry, SRM Institute of Science and Technology, Kattankulathur, Tamil Nadu 603203, India. E-mail: karthiks13@srmist.edu.in, kart@mine.kyushu-u.ac.jp*
[c] *Department of Earth Resources Engineering, Kyushu University, Fukuoka 819-0395, Japan*
[d] *Departamento de Ingeniería Mecánica, Facultad de Ingeniería, Universidad de Tarapacá, Avda. General Velásquez, 1775, Arica, Chile*
[e] *eInstitut de Recherche d'Hydro-Québec 1806, boul. Lionel-Boulet, Varennes, Québec, J3X 1S1, Canada*

Brahmari Honnappa

Ms Brahmari Honnappa is currently pursuing her PhD in the Department of Physics and Nanotechnology at SRM Institute of Science and Technology. She completed her MSc in Materials Science in 2020 and BSc in 2018 from Mangalore University, Mangalore, Karnataka. Her research focuses on the development of novel catalysts, along with the synthesis of novel nanocomposites and low-cost materials for electrochemical hydrogen evolution reactions.

Sathya Mohan

Ms Sathya Mohan is currently pursuing her PhD in the Department of Chemistry at SRM Institute of Science and Technology. She has completed her MSc in 2020 from SASTRA University, Thanjavur and BSc in 2018 from Bharathidasan University, Trichy, Tamil Nadu. Her research interest includes degradation of pharmaceutical waste by synthesising novel chemo-bio photocatalysts.

1. Introduction

The world is growing faster as a result of increased energy access for inhabitants, cleaner fuel, and the growing penetration of renewables. Constructing a sustainable and cleaner energy resource to concurrently meet the current as well as future demands is one of the most pressing challenges. Towards this, initiatives are being taken globally to boost the progress as well as the application of renewable energies, which comprise the solar energy, wind energy, and hydel energy.[1] Correspondingly, as proposed by Bockris *et al.* in 1970,[2] the term ''hydrogen economy'' is deemed as among the cleanest and enticing utilisation techniques with the output being nothing more than water. We can produce clean hydrogen by splitting water using renewable energy sources, which are then collected, stored, and used for a variety of other purposes, such as the production of ammonia, fuel cell electric vehicles, coke/iron production, refining processes, and human needs.[3–5] However, electrochemical methods are rather discovered to be the most straightforward, practical, and successful strategies for hydrogen evolution as compared to the conventional reformation of steam or gasification with coal. Based on reactions between fossil fuels and steam or other renewable methods, one of the most captivating and non-carbon-emitting methods for producing hydrogen, is water electrolysis.[6–8] The goal of obtaining a significant amount of H_2 on a large scale remains an obstacle, and thus this solution is still incomplete.[9–11] Hydrogen fuel cells based on membrane technologies, which are considered the state-of-the-art technology for H_2 methodologies and studies, are another way of harvesting clean energy at a low temperature,[12–14] nevertheless, electrolysis is one of the easiest harvesting ways to extract clean and green fuel, which is efficient and effective for future technologies;[15] thus, the target is drawn back with the fabrication of an electrocatalyst, which is efficient and cost-effective due to lacklustre kinetic parameters to accelerate the reaction.[16] The research community

Mariyappan Shanmugam

Mr Mariyappan Shanmugam is currently pursuing his PhD in the Department of chemistry at SRM Institute of Science and Technology. He completed his MSc chemistry from SASTRA University in 2019 and BSc chemistry in 2017 from Bharathidasan University, Tamil Nadu. His research interest is in the development of novel Metal–Organic frameworks (MOFs) for photocatalytic hydrogen production from water.

Ashil Augustin

Mr Ashil Augustin is currently pursuing his PhD in the Department of chemistry at SRM Institute of Science and Technology. He completed his MSc chemistry from Bharathidasan University, Tamil Nadu in 2020 and BSc chemistry in 2018 from Mahatma Gandhi University, Kerala. His research focuses on the development of novel Organic-Inorganic hybrid materials for photocatalytic hydrogen production from water.

Prince J. J. Sagayaraj

Ms Prince Jemima Jebaselvi. S is currently doing her PhD in SRM Institute of Science and Technology, Kattankulathur. She completed her Post Graduate in Chemistry at Loyola College, Chennai and Undergraduate in Chemistry at Stella Maris College, Chennai. Her field of interest is in designing and developing earth abundant materials as photocatalysts for solar fuel production, HER and sustainable energy development.

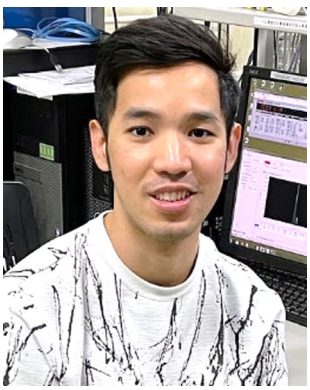

Chitiphon Chuaicham

Dr Chitiphon chuaicham is a special assistant professor at Earth Resources Engineering, Kyushu University, Japan, in the group of Professor Keiko Sasaki. He is studying photocatalysis based Advanced Oxidation Processes for the decontamination of waste water. He received his doctoral degree in engineering from Kyushu University in 2019, where he studied photocatalysis for waste water treatment. He received his BSC and MSc in Chemistry from Mahidol University, Thailand. His research interests focus on the development of two dimensional (2D) materials and natural materials for photocatalysis, and their applications in energy and environment purposes.

has been striving for a solution to design an electrocatalyst that is reliable, environmentally friendly, and cost-effective. There are basically two ways to increase the catalytic activity to tackle this issue.[17–19] Either to increase the superficial activity of the total electrode *via* morphological variation or/and to improve the activity at every active site of the electrode by engineering the composition.[16,20–22] To meet these two goals and to formulate a profound electrocatalyst for HER and due to their numerous surface sites that remain active and also because of quantum confinement, quantum dots are one such material, which when designed into a composite, makes for dependable future electrocatalysts. Our review focuses on the transition

Saravanan Rajendran

Dr Saravanan Rajendran received his PhD in Physics – Material Science in 2013 from the Department of Nuclear Physics, University of Madras, Chennai, India. He was awarded the University Research Fellowship (URF) during the years 2009–2011 by the University of Madras. He was awarded SERC and CONICYT-FONDECYT postdoctoral fellowship by the University of Chile, Santiago, Chile, in 2014–2017. Currently, he is currently working as an Assistant Professor in the Faculty of Engineering, Department of Mechanical Engineering, University of Tarapacá, Arica, Chile. He has been Editorial Member and Guest Editor of several reputed international journals. His research interests focus in the area of nanostructured functional materials for renewable energy and wastewater purification. He has published in >110 (~9600 citations) international peer-reviewed journals.

Tuan K. A. Hoang

Dr Tuan Hoang received his PhD in Chemistry in 2011, from the Department of Chemistry & Biochemistry, the University of Windsor, Canada. His PhD work focused on the development of novel hydrogen storage material functioning via weak chemisorption. During 2012-2013, he was a Research Associate in the School of Chemistry, University of Glasgow. In 2014-2018, he worked for Positec Group and the University of Waterloo where he solved problems during the scaling up of rechargeable batteries for use in tools, devices, and cars. He joined the research institute of Hydro-Québec, where he is currently holding a senior research position. He has published about 80 research papers and two patents in hydrogen technologies and rechargeable batteries.

Keiko Sasaki

Prof. Keiko Sasaki received her PhD in 1997 from Hokkaido University, Japan. She is currently a full professor in Department of Earth Resources Engineering, Kyushu University and a coalition member of Science Council of Japan. She is leading the Geomimetic Material Science for Environmental Remediation. Her research interest is to develop advanced materials using natural and artificial minerals for environmental remediation. She has published >200 research papers in prestigious journals, including Journal of Materials Chemistry A, ACS Sustainable Chemistry Engineering, Environmental Science and Technology, Journal of Hazardous Materials, and Chemical Engineering Journal.

Karthikeyan Sekar

Dr Karthikeyan Sekar currently working as an Assistant Professor, at SRM Institute of Science and Technology, India. Previously he worked as Special Researcher at the University of Tokyo, Japan. He has received prestigious JSPS Invitational Fellowship 2022, and the Royal Society Newton International Alumni Grant 2021. Before that he has received the JSPS Postdoctoral Fellowship, Japan (2018 to 2020), and the Royal Society Newton International Fellowship (2016 to 2018), UK. He was also awarded the Fellow of higher education academy, United Kingdom (2018) and Malaysian International Scholarship (MIS, 2015), Malaysia, Senior Research Fellowship 2012 from CSIR, India, and International Travel Grant 2012 from DST, India. His research interest is towards the development of biomass derived carbon-based materials used as catalysts for energy and environmental applications. He has published 80 research articles, and four patents.

metal-based quantum dot composites as proficient electrocatalysts for electrochemical HER. This review provides considerate and comprehensive insights that cover the HER, focusing in particular on the acidic and alkaline medium electrolytes used in the reaction and the underlying mechanistic pathway. Moreover, the recent development of TMQDs as an effective electrocatalyst is discussed, as well as the comprehension of their activity due to their composition, structure, and active sites available for the reaction to proceed, along with future perspectives and challenges.

2. The reaction of hydrogen evolution (acidic and alkaline medium)

Electrochemical water splitting involves the concurrent usage of water in order to produce hydrogen and oxygen. It looks like a simple solution for transforming electrical energy into chemical energy.[8,23,24] In an electrocatalytic HER, H_2 is obtained after the reduction of the proton (H^+) or H_2O at the interface of an electrode and electrolyte (redox reaction), which entails a series of simple steps that are solely based on electrolyte pH. The overall HER reaction is a simple process of water being split into hydrogen and oxygen but the entire electrochemical process is not that simple, involving a multi-step process on the electrode surface. This is because, at higher current density, there can be significant ohmic losses due to ineffective ion transportation in the electrolytic solution. To control this effect, it is necessary to use highly conducting electrolytes. Thus, the two most conductive ions H_3O^+ and OH^- are to be utilized in the electrolysis processes either in highly acidic or highly basic medium (Fig. 1).

Though commercial applications work in any of the mediums, the usual outlook has been to focus on the acidic medium because it will have greater potential and have higher conducting nature.[26] The kinetics of the reaction depends on the material used in the electrode, for example, platinum is the renowned material for the hydrogen evolution reaction, whereas a mercury electrode has slower kinetics. Other parameters include electrode orientations (*e.g.*, amorphous surface, polycrystalline, single crystal) and the nature of the electrolyte. Table 1 gives the overall idea about the HER reaction mechanism occurring in acidic and alkaline mediums. To put the entire mechanism in a nutshell, the hydrogen evolution begins on the surface of the catalyst by adsorbing the H atom, which is the Volmer reaction. Further, based on the nature of electrocatalysts, the reaction can proceed in two ways, which are with two adsorbed H, the Tafel reaction, or single adsorbed H, the Heyrovsky reaction; thus, facilitating the liberation of the H_2 molecule. Hence, it is important to have a good choice of electrocatalyst for the reaction, which can give good adsorption of H.

2.1. Understanding the mechanistic approach of acidic HER

Water electrolysis in an acidic medium is the cathodic reaction where the hydronium ions get reduced to hydrogen gas. Considering thermodynamics, the reaction occurs at a potential that is equal to that of the reference hydrogen electrode (RHE) reaction occurring, initially with proton reduction at the active catalyst site – Volmer step, followed by the molecular hydrogen evolution, which is through the second electron/proton transfer – Heyrovsky step and if the recombination of adsorbed protons occur that is the Tafel step (eqn (1)–(3)).

$$H_3O^+ + e^- + * \rightarrow H^* + H_2O \quad (1)$$

$$H^* + H_3O^+ + e^- \rightarrow H_2 + H_2O \quad (2)$$

$$2H^* \rightarrow H_2 \quad (3)$$

Here, * signifies the surface-active sites, and H*, the active sites with an adsorbed hydrogen. Generally, a single step sets back the kinetics of the reaction that is electrochemical in nature. This step is considered the rds (rate determining step).

In electrochemical hydrogen evolution, many reports focus on the surface of the Pt in an acidic medium for the mechanism of the reaction (eqn (4)),

$$H^+ + e^- + Pt^* \rightarrow Pt - H_{UPD} \quad (4)$$

Nicolas *et al.*,[28] explained that there are basically 4 regions for a platinum catalyst appearing as polycrystalline (Pt(pc)) in a typical CV in the acidic medium (Fig. 2). The first one with

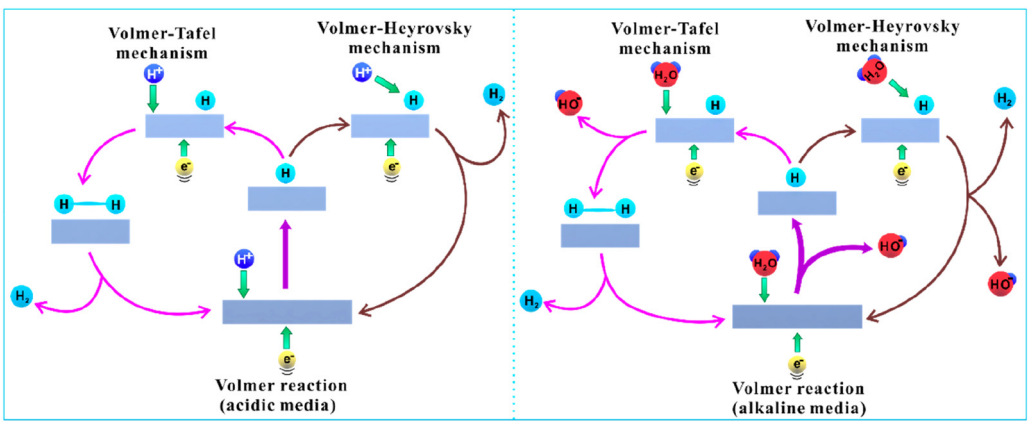

Fig. 1 Generalized mechanism of HER in acidic and alkaline medium. Reproduced from ref. 25 (Copyright 2019, American Chemical Society).

Table 1 HER mechanism in acid and alkaline conditions[27]

	Acid	Alkaline	Tafel slope
Volmer	$M + H^* + e^- \rightarrow M - H$	$M + H_2O + e^- \rightarrow M - H + OH^-$	$b = 2.303RT/(\propto F) \approx 120$ mV dec^{-1}
Heyrovsky	$M + H^+ + e^- + M - H \rightarrow H_2 + M$	$M + H_2O + e^- + M - H \rightarrow H_2 + OH^- + M$	$b = 2.303RT/((1 + \propto)F) \approx 40$ mV dec^{-1}
Tafel	$2M - H \rightarrow H_2 + 2M$	$2M - H \rightarrow H_2 + 2M$	$b = 2.303RT/(\propto F) \approx 30$ mV dec^{-1}
Overall	$M + 2H + 2e^- \rightarrow H_2$	$M + H_2O + 2e^- \rightarrow H_2 + 2OH^-$	

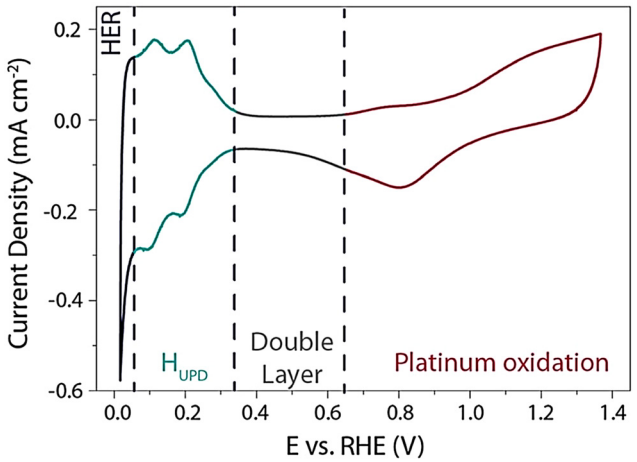

Fig. 2 Cyclic voltammogram of Pt(pc) electrode at scan rate of 50 mV s^{-1} in an electrolyte solution of 0.5 M H_2SO_4 solution which was degassed in argon. Reproduced from ref. 28 (Copyright 2019, The Royal Society).

potential >0.65 V *vs.* RHE is the area for surface oxidation/reduction of Pt leading to aggregation of Pt–OH or/and Pt oxide on the Pt surface due to the specific adsorption of anions.

The second region is the potential in the range of 0.35 V and 0.65 V *vs.* RHE, the region of no faradaic process occurrence referred to as a "double layer region." The third one is the hydrogen underpotential deposition (H_{UPD}) region in the potential 0.05 V and 0.35 V *vs.* RHE. The proton discharge from the surface of Pt occurs in the final region at the higher negative potential, and hydrogen gas is evolved.[29–31] The H_{UPD} region is distinguished by a single broad envelope and a couple of redox peaks at around 0.2 V *vs.* RHE, followed by the peaks at around 0.1 V *vs.* RHE.[28]

Nørskov *et al.* gathered the experimental data on the HER in 2004 for various metals, by utilization of Density Functional Theory (DFT) that corresponds to adsorption energies by presenting the modern volcano plots.[32] The findings explain the Pt's superior activity in HER as well as provide an insightful explanation of HER's activity and its dependence on hydrogen binding energy.

In Fig. 3, the volcano plot shows an overall idea of the choice of electrocatalysts. Basically, Pt is the current benchmark material, but considering the TMQDs, the widely studied material is MoS_2 QDs, the reason lies with the bases on a close-to-neutral ΔG°_H of MoS_2 edges, which has later been established with experiments. The edge sites of MoS_2 could have high HER activity as a successful pattern.[36–38] Further, more research has been conducted and advanced in HER catalyst, emphasizing the theoretical and practical progression for the same.[39]

2.2. Understanding the mechanistic approach for alkaline medium

HER in alkaline medium is critical and important as it is a popular technology within the industrial sector, and can perform an important role in treating discharged alkaline water as alkali and chlor-alkali electrolyzers.[40] The reports to date have no alternative to Pt when studied under an alkaline medium on efficiency grounds.[41] Thus, the pathway of the reaction must be understood and validated using the basic laws of electrode kinetics, paving the way for the development of efficient electrocatalysts.[42] It is also crucial to have HER activity as

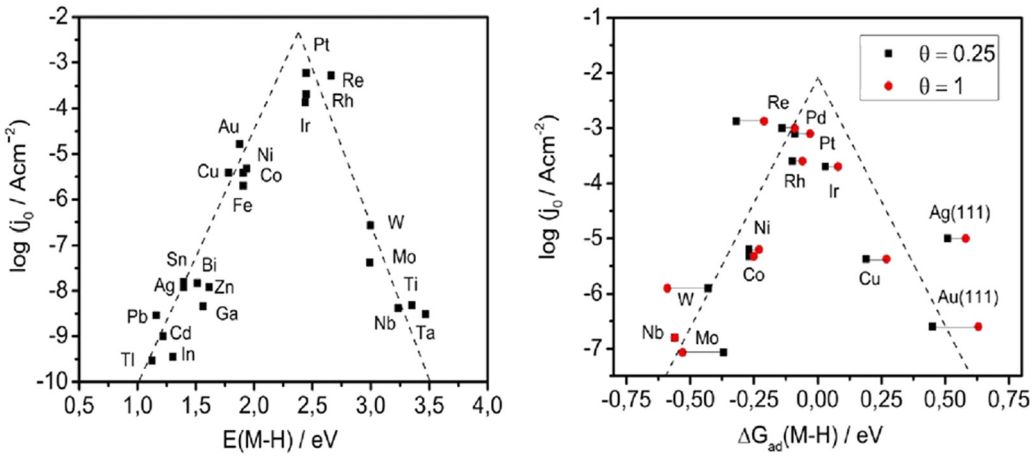

Fig. 3 (a and b) The "volcano" plot by Trasatti[33] from experimental and the "volcano" plot derived from DFT by Norskov *et al.*[34] Reproduced from ref. 35 (Copyright 2016, John Wiley & Sons).

inclusion with the viewpoint of designing a catalyst and to improve the rate-determining step mechanistically, for the reduction–reaction potential with improved HER activity.[43,44] As a well-established fact, there is water adsorption, hydrogen binding energy, water dissociation and OH^- adsorption, which influence the HER activity. Nonetheless, the reaction mechanism is well accepted, and computational chemistry has largely been neglecting the theory-based negotiations on the topic of energetics and kinetics of the HER in the alkaline medium that constantly remains in debate among chemists.[45] Though many electrochemical reports report distinct aspects of the HER mechanism, the metal–H_{ad} bond energy[33,46–48] for the reaction, mostly used for the description is insufficient to elaborate the lower activity in basic media. From the mechanism of HER, for the whole catalytic activity, the dependence of pH of the catalyst underpins that it remains a debate.[49] Conway *et al.* explored the characteristics of UPD and OPD (under and over potential deposited) on H over the Pt surface based on the energy of the bond and exchange current density corresponding to the chemisorbed hydrogen atoms over the metal or stand Gibbs energies of the chemisorption of 2H from H_2, *i.e.*, the volcano relation.[51,52] It was found that kinetically important intermediate is being adsorbed on the Pt or other metals being utilized in HER activity is due to the weakly bound H of OPD rather than strongly bound H of UPD, which means higher the OPD H, the activity is also eventually higher. Under basic conditions, the coverage of hydrogen atoms of OPD is fairly lower in comparison with the acidic medium, hence resulting in the slower reaction rate.[53] The reaction mechanism for alkaline HER underlies from the point that at the potential of −1000 mV, HER is observed,as shown in Fig. 4. H_2 desorption and desorption from the surface of the electrocatalyst lies between the potential of −500 mV to 0 mV. The OH adsorption or the Pt oxidation lies in the potential of 0 V–750 mV and a further increase in the positive potential leads to the oxygen evolution reaction (OER). The cyclic voltammogram clearly indicates that the reaction occurring on the polycrystalline Pt electrode surface is hydrogen evolution with clear peaks indicating the H adsorption and desorption at a particular potential. Moving towards the computational aspect, the studies for alkaline HER are still very limited due to inadequate data about the electrode potential and the pH that are dependent on the kinetics of water dissociation and thermodynamic hydrogen adsorption processes.[54]

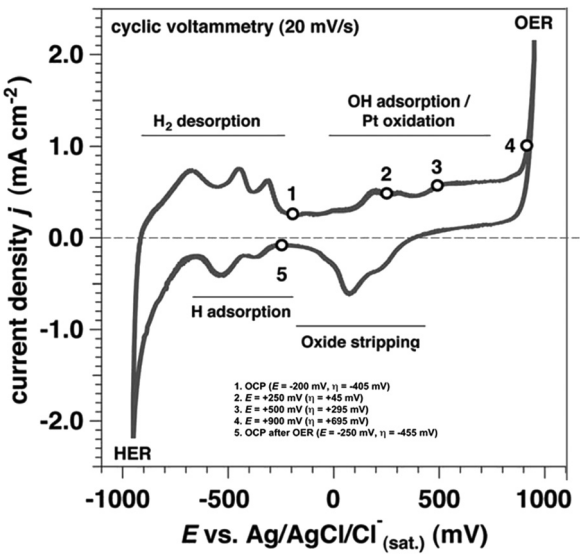

Fig. 4 Cyclic Voltammogram of polycrystalline Pt electrode with a rate of scanning equivalent to 20 mV s^{-1} in an electrolyte solution of 1 M KOH solution. Reproduced from ref. 50 (Copyright 2017, The Royal Society).

3. Choice of transition metal quantum dots as electrocatalyst

The performance of the electrochemical hydrogen evolution reaction depends on various factors starting from the electrocatalyst, environmental conditions, electrolyte solution, which is pH dependent, and so on. Amongst the mentioned factors, the choice of electrocatalyst plays a prominent role in determining the efficiency of the material, which in turn determines the hydrogen evolution. To achieve, higher hydrogen evolution along with cost efficiency, an electrocatalyst should have good compatibility, abundant in nature, and should have efficient working in a wide pH range.

The benchmark catalysts such as Pt or Ru also have drawbacks, such as cost and availability. Numerous earth-abundant catalysts with good activity have been reported to date. In consideration of HER, transition metals have been extensively studied as transition metal dichalcogenides, transition metal carbides, transition metal nitrides, phosphides, and so on. Recently, a variety of materials are studied as active catalysts for electrocatalyst properties.[55,56] Amongst all of these materials, the transition metal quantum dots have enhanced properties such as increased surface area, a higher surface-to-volume ratio, fluorescence properties, and conductivity, together contributing to an exemplary activity of these materials in the electrochemical hydrogen evolution reaction.[57–59]

3.1. Transition metal quantum dots: synthesis and their application in HER

Quantum dots (QDs), in general, nano-sized semiconductor crystals, have found fascinating applications in numerous scientific fields. In 1980, Russian Physicist, Alexei Ekimov first discovered QDs.[60] Essentially, Bohr's radius of the group II–VI or III–V-based materials is larger than their physical dimensions.[61] After more than two decades of its introduction into research, its usability has increased.[62,63] Quantum confinement effect and controllable fluorescence emission properties of QDs have been extensively studied initially, which was applicable in the field of biosensing and bioimaging.[64,65]

Quantum dots do have a broad range of unique optical, electrical, physical, and chemical properties, with their applications in illumination, energy harvesting, biology, medicine, sensors, cameras, displays, and communication and information technology. QDs are often used to build displays, effective

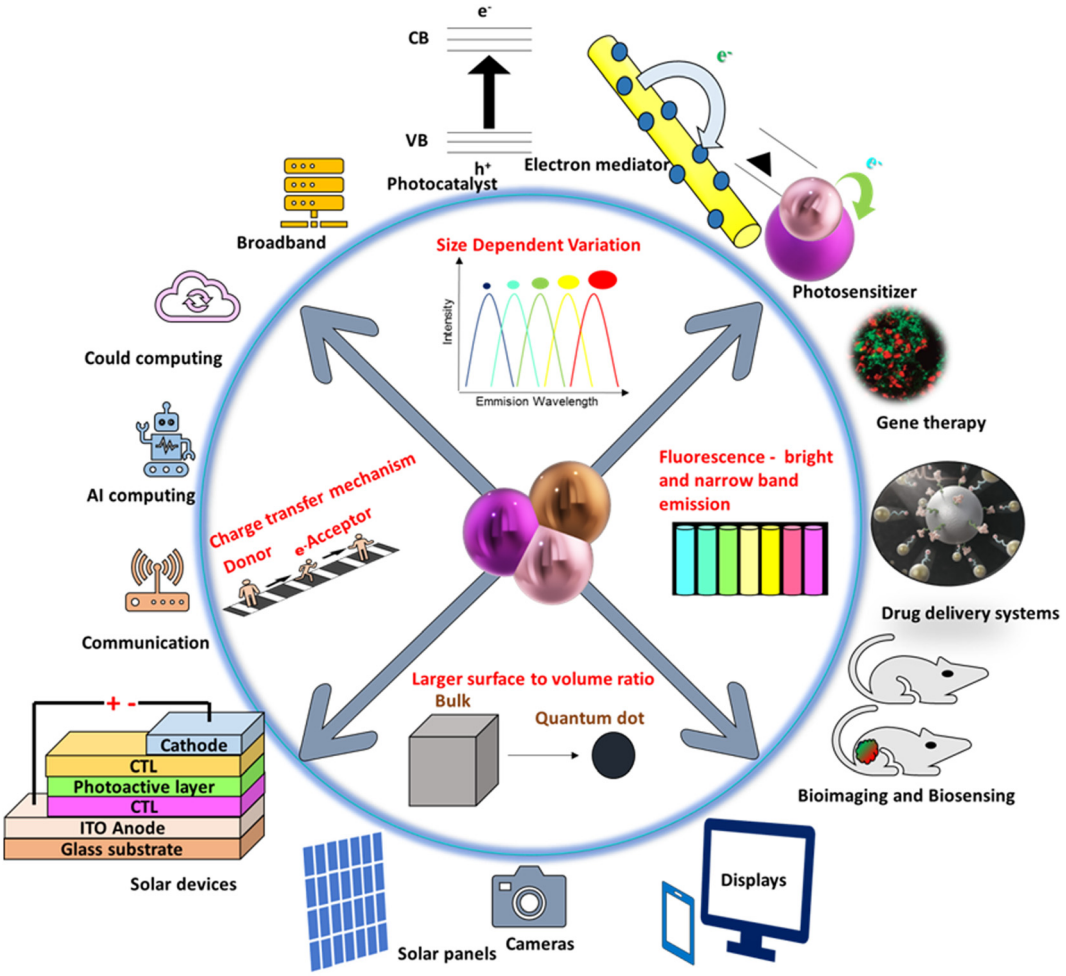

Fig. 5 Progress in quantum dots for a wide range of applications; there are still opportunities for the configuration of QD-enabled new device architectures, a few of which are listed here.

lasers, solar harvesting devices, and biotags that are now on the market, and they continue to gain attraction in sensing, quantum information, and photovoltaics. Anisotropic geometry and confinement effects in QDs are utilized in a wide variety of applications (Fig. 5) such as photochemical reagents,[66] light emitting diodes,[67] catalysis,[68] solar cells,[69] due to their properties such as photochemical,[70–72] magnetic,[73–76] optoelectrical,[77–79] piezo-electrical.[80–83] QDs with enhancing properties exhibited by the semiconductors are proved to be effective electrocatalysts in HER in the current research. Predominantly, due to a reduction in size, the metallic materials will have a wider surface area, less mechanical fracture, and larger active sites, amidst the above attractive characteristics, metallic QDs lack good electrical conductivity and have a higher tendency to agglomerate,[84,85] thus making them inefficient as a single-component electrocatalyst, but QDs effectively work when they are engineered in composites. These composites have been widely manipulated in research as efficient electrocatalysts.[86]

3.2. Synthesis and properties of TMQDs

Among the many methods proposed for the synthesis of QDs, the broad classification includes ''Top-down'' and ''Bottom-up'' approaches (Fig. 6), and the properties are modified with the

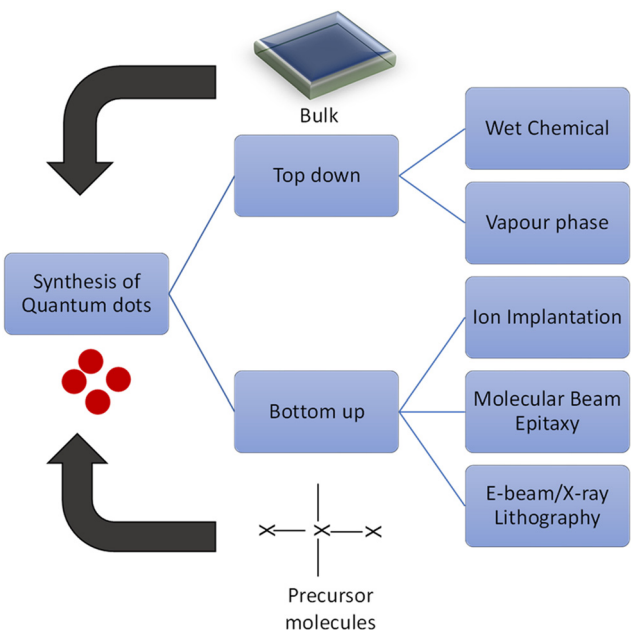

Fig. 6 Different approaches for the synthesis of quantum dots.

preparation methods or post-synthesis treatments.[87] Top-Down approaches include molecular beam epitaxy (MBE) for thin film deposition, X-ray, and electron beam lithography or ion implantation techniques. The other bottom-up methods include chemical reduction with self-assembly in the solution.[88–90] The top-down approach to the synthesis of QDs involves nothing but a process in which a bulk semiconductor is bought down to a diameter of approximately 30 nm range by systematically controlling the reaction atmosphere, thus achieving materials with a quantum confinement effect. Such materials have a controlled size and shape with exceptional packing geometries.

There are similarly other methods for synthesis of QDs, but the major disadvantage is the incorporation of impurities and structural imperfections that arise during the process.[91]

Lasek *et al.* have successfully synthesized transition metal tellurides in an ultra-high vacuum MBE chamber by co-deposition of the transition metal and tellurium with the highly oriented pyrolytic graphite (HOPG-) or MoS_2 substrates (van der Waals substrate).[92] Bouravleuv *et al.* utilized the MBE route on the semi-insulating and n-type GaAs(001) substrates synthesizing $Al_xGa_yAs_z$ quantum dots with selective doping of Mn.[93] Thevuthasan *et al.* synthesized Au nanocrystals with ion beam implantation.[94] Ueda *et al.* synthesized InAs QDs by sequential implantation as in a-SiO_2.[95] Weiwei Chen *et al.*[96] successfully synthesized $CsPbCl_3$ quantum dots by understanding the Palazon's group's synthesis of $CsPbX_3$ QDs surface *via* the X-ray lithography route, resulting in enhanced stability of the synthetic QDs.[97]

To date, the most pronounced synthesis of QDs follows the bottom-up method, which is broadly divided into vapour-phase and wet-chemical methods.[91] In the vapour-phase method, the QDs are built from atomic processes. Basically, no pattern is observed in the self-assembled molecules.[98–101] In the self-assembly process the MBE, sputtering, or aggregation of monomers, are also categorised.

Forleo *et al.* synthesized ZnO quantum dots by using the zinc acetate as a precursor, which was performed at room temperature, making the possibility of attaining uniform-sized QDs with enhancement from the application point of view.[102] Hui Zhang *et al.* successfully confirmed the synthesis of CdS quantum dots doped over Mn, Cu, and Ni with bi-metallic clusters for gram-scale synthesis under mild reaction conditions.[103] Currently, the wet chemical method is applied widely to control various factors of the changes in the properties of the materials.

A typical quantum dot is one in which the structural orientation has a metalloid crystalline core and this core material is known to be encapsulated or engulfed within a thin shell form. This is usually performed to enhance the electronic and optical properties of the quantum dots themselves. Examples of such metalloid crystalline cores include CdS, CdSe, or CdTe and the thin shell is composed of transition metals such as ZnS. In general, the quantum dots possess properties that prominently depend on the particle size and chemical composition of quantum dots.[104] It is evident from an MQD system that a non-metallic atom with enhanced electronegativity is preferably selected to passivate the MQD active sites efficiently.[105] Mei *et al.* in 2019 discussed the enriched optical properties that are colour tuned, made of cadmium-free transition metal ions that are doped with InP/ZnS quantum dots. This work inculcated a nucleation doping method *via* an organic synthetic pathway wherein a series of transition metals co-doped with InP/ZnS quantum dots with variable colour-tuned optical properties were synthesized. From the resultant PL spectra of the transition metal-co-doped quantum dots, it is known that all the QDs possess color-tunable dual emissions and indicates that the dopant emission is predominantly due to the doping of Cu whilst that of Mn.[106] To be more precise, MQD has enhanced physical, chemical, and various other mechanical properties in comparison with those of the 2D materials that include sulphides and selenides of metals. This enhancement of properties is basically due to their larger surface area, edge-effect, and quantum confinement effect being lower. At the near Fermi level, the MXQD possesses increased metallic conductivity and have more electron density, which is attributed to the small size of the material itself. This property of electrical conductivity can be furthermore increased by doping of any heteroatom or by the synthesis of carbonitrides or nitrides of quantum dots. One preferable advantage of enhancing the electrical conductivity of MQD is that they tend to uplift the processing of electron transfer, which in turn attributes to the creation of more active sites.[107] TMQDs including carbides, oxides, and nitrides are generating wide attention due to their vast range of properties. These include conductivity, high active sites, cost-effectiveness, good dispersion ability, biocompatibility, tuneable framework, remarkable optical properties, and functionalization with different groups. The use of MQDs for the heterostructure composite is a strategy to tune the band gap and improve the catalytic efficiency.[105] Mo_2C QDs and WC QDs incorporated with N-doped graphene nanosheets have been reported for HER. The catalyst shows good durability and high exchange current density. Ti_3C_3 Mxene QDs show more grain boundaries and edge defects than the 2D Mxene perfect crystal. The use of OsO_x quantum dots with graphydine has been recently reported as an electrocatalyst for HER under visible light irradiation. The progress in the field of MQDs is in the growing stage in the field of HER. TMQDs and their surface modifications for improved catalysis. Furthermore, it is important to understand the clear mechanism from experiments, followed by theoretical data to enhance development in this field.

3.3. TMQDs in electrochemical HER as an efficient electrocatalyst

Transition metal quantum dots have gained increasing attention recently due to their tuneable characteristics in both optical and electronic stands.

In comparison with the semiconductors which are used traditionally over the years, the layered transition metal dichalcogenides show significantly better properties of fluorescence when they are confined into quantum dots.

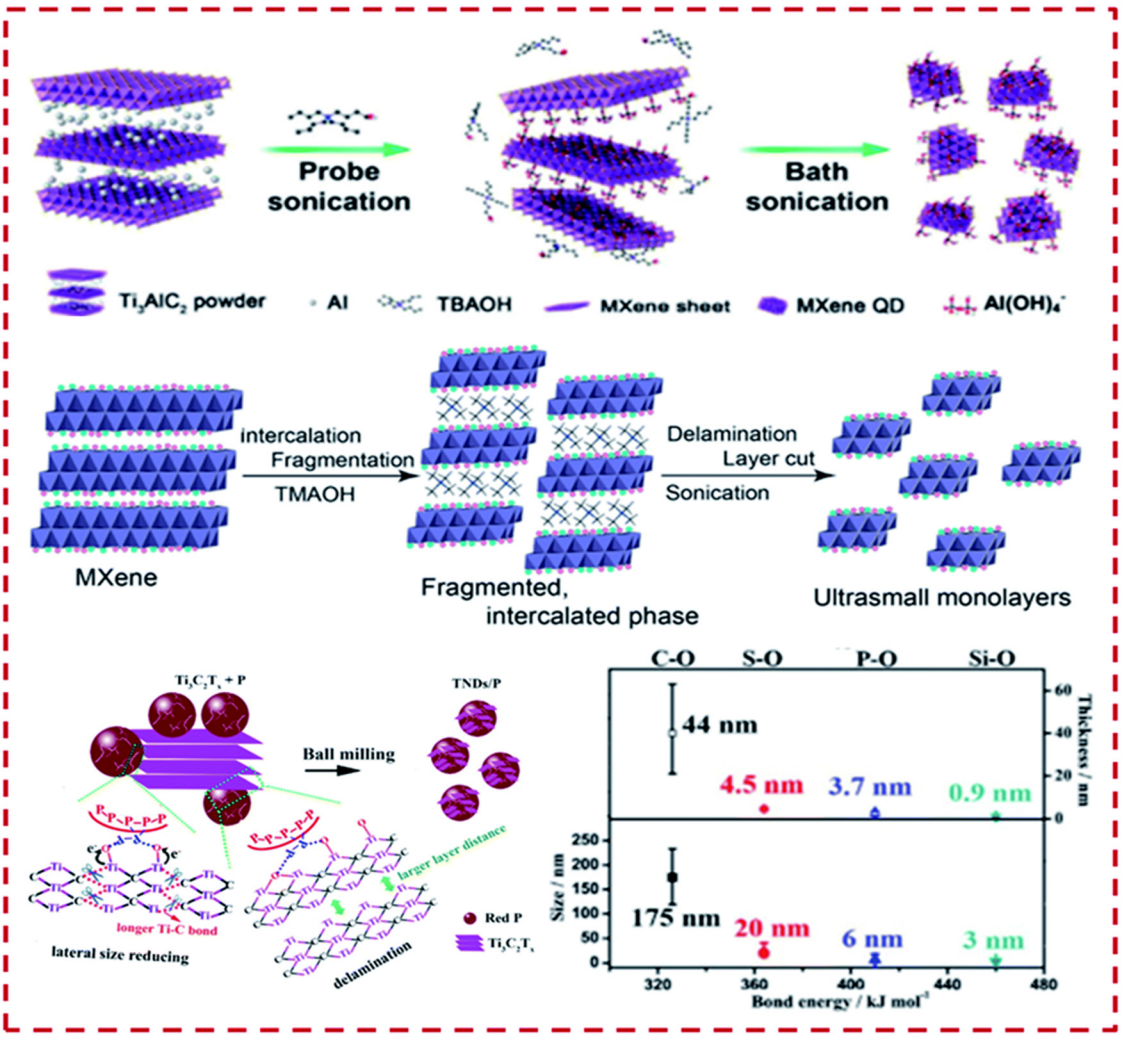

Fig. 7 Schematic representation of the synthetic methodology of Ti_3C_2 QDs involving a double step ultrasound method. Reproduced from ref. 109 (Copyright 2020, The Royal Society).

In the field of bio-sensing and bio-imaging, TMQDs are proving themselves as efficient candidates primarily due to their high dispersibility and extremely low toxicity.[108]

It is known that when the bulk layered transition metal dichalcogenides are reduced to quantum sizes, they tend to show enhanced properties, which is due to the quantum confinement effect and the prominently grown-up edges. Research studies reveal that the metal quantum dots of zero dimensions are known to have increased the surface-to-volume ratio, which means that the exposed edges are larger in proportion and the chemical and physical properties are largely tuneable possessing profound solubility when dissolved in aqueous solutions.[110]

Shao *et al.* in 2020 emphasized the synthesis and application prospectus of 2-dimensional transition–metal-based MXenes that are driven out into quantum dots *via* fragmentation into ultra-small layers by utilising the technique of sonication (Fig. 7).[109]

Huang *et al.* observed the controlled construction of hetero-structure with ultrafine MoS_2 QDs, which were decorated on the $Ti_3C_2T_x$ MXene nanosheets (MQDs/$Ti_3C_2T_x$) (Fig. 8).[111] With the optimisation study, the lowest onset potential of 66 mV was obtained with a Tafel slope of 74 mV dec^{-1}, which is small with increased life showing contrast behaviour of individual Mxene or QDs.

Liu *et al.* reported the introduction of transition metals onto the Ru metal-based carbon quantum dots. In this method, transition metals such as Ni, Mn, and Cu are doped over the ruthenium lattice and the electrochemical production of hydrogen is studied.[112] To be precise, the nickel doped ruthenium carbon quantum dots show low overpotential of about 13, 58, and 18 mV that achieves a current density of about 10 mA cm^{-2} in solutions of 1 M KOH, 0.5 M H_2SO_4, as well as 1 M PBS. (Fig. 9a–e).

Experimental reports suggest that the excellent activity of the Ni-based catalyst is largely due to its selectivity towards crystalline surface of the hcp RuNi particles and its variation in the electronic structure after the doping of transition metal. Ou *et al.* formulated a facile and a generally-extremely fast laser ablation technique in order to synthesize MoS_2 quantum dots

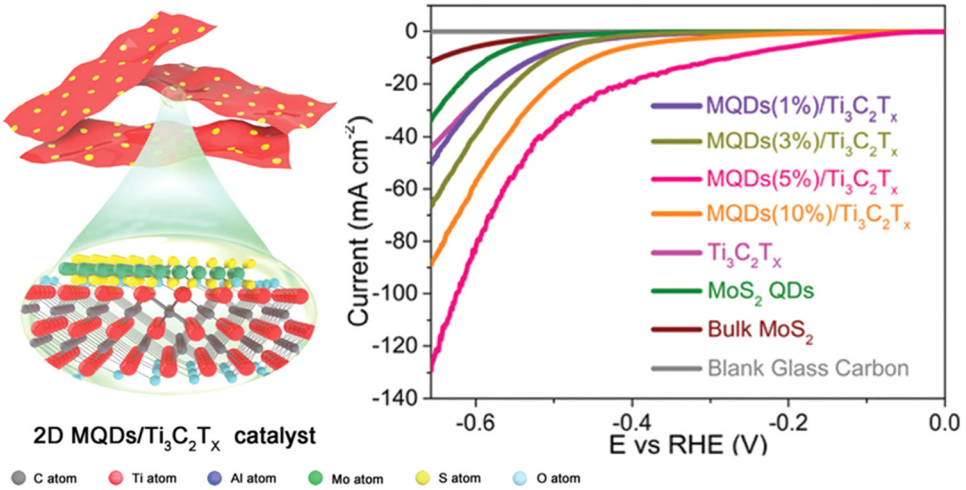

Fig. 8 The overall graphical representation of HER with MoS_2 QDs with MXene composite. Reproduced from ref. 111 (Copyright 2022, The Royal Society).

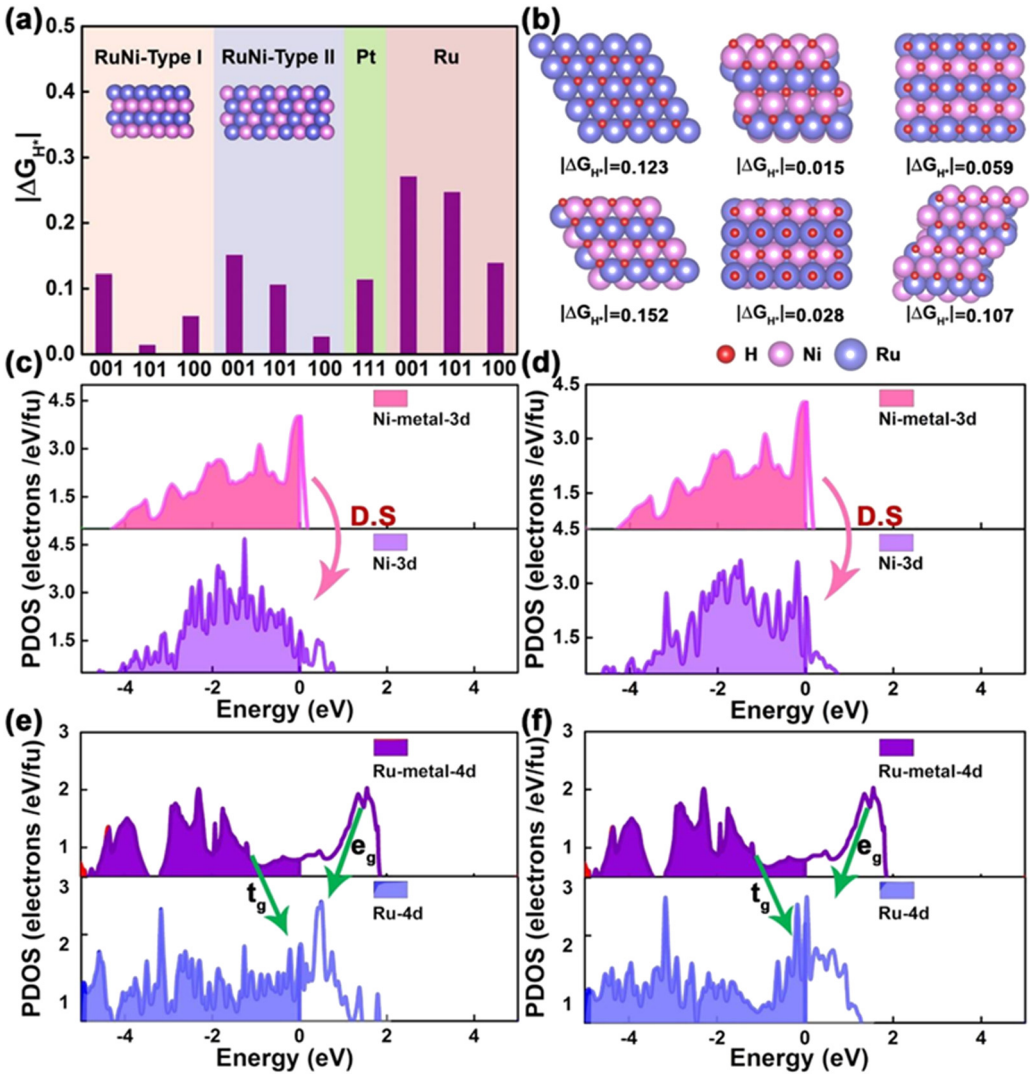

Fig. 9 Enhanced activity of the attributed to the energies of the adsorbed energies (a), crystal structure (b), partial density of states (c–f). Reproduced from ref. 112 (Copyright 2020, John Wiley & Sons).

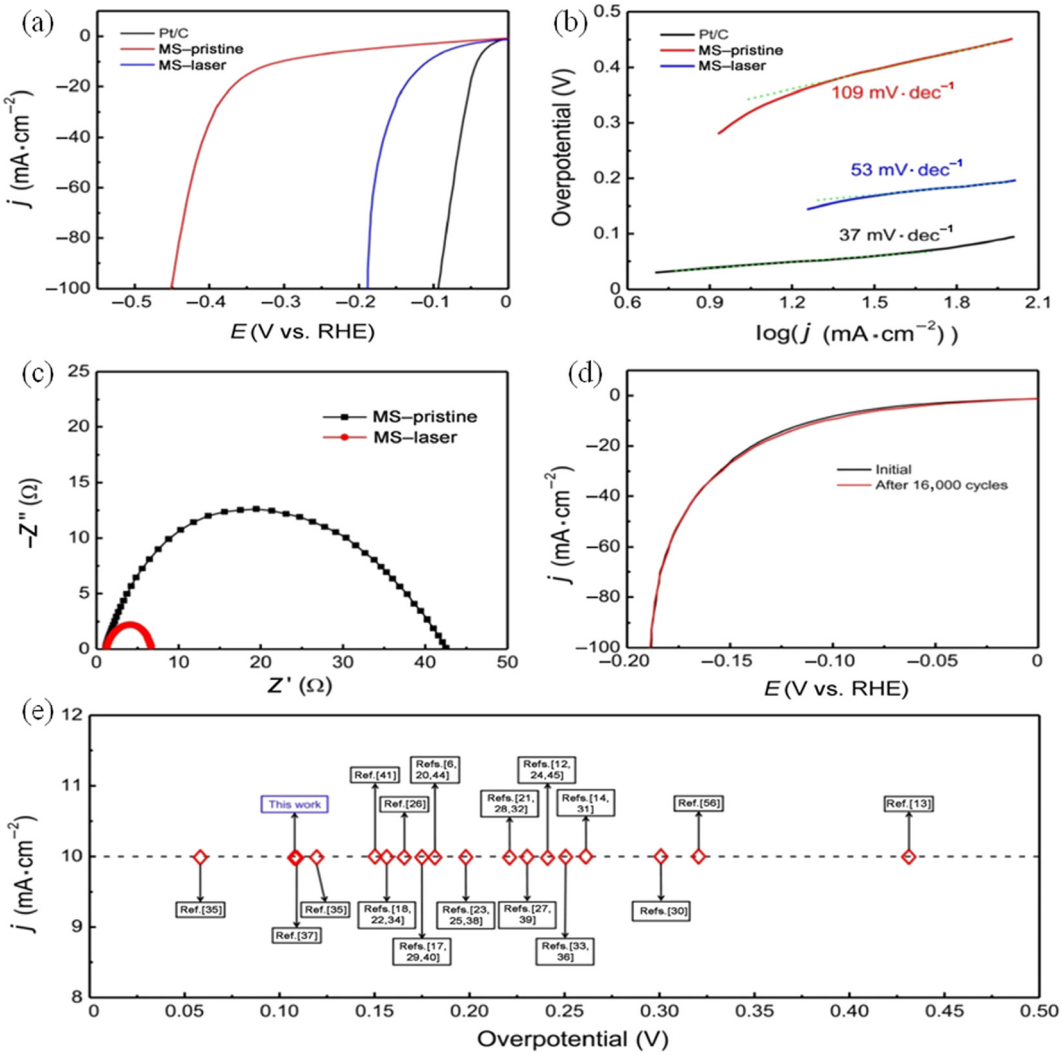

Fig. 10 Electrochemical studies as polarisation curves before (b) and after (d), Tafel slope (b), Nyquist plot (c) and stability (e) of MS-QDs compared with bulk MoS_2. Reproduced from ref. 113 (Copyrights (2022, Springer Nature)).

possessing a higher number of active sites along with upskilled conductivity of electrocatalytic HER.[113] The electrochemical analysis of the prepared sample MoS_2 was compared with that of the pristine MoS_2.

The results are in accordance with the improved active efficiency of the MoS_2 catalyst. After ultrafast ablation treatment at a 100 mA cm^{-2} current rate, it was evident that the overpotential was decreased from 450 mV to 187 mV. From the above results, the team found that the overpotential values of pristine MoS_2, MoS_2, and the commercially available Pt/C were known to be 345, 108, and 38 mV, respectively (Fig. 10a–e). This material tends to show an overpotential value that is very much closer to the commercially available Pt/C. This high performance of the MoS_2 quantum dots has been acknowledged, thanks to the improved specific surface area, as well as enlarged active sites in addition to good conductivity and high hydrophilicity. Xianpei *et al.* designed a novel method of increasing the efficiency of the electrocatalyst for hydrogen evolution by synthesizing MoS_2 nano-catalyst, which is of ultra-small size and has few layers, that can enhance the activity of the catalyst (Fig. 11a).[114]

This preparatory method could be facilitated by a hydrothermal synthesis route. Comparative electrochemical studies of the MoS_2 catalyst with that of the bulk MoS_2 and the commercial Pt electrode reveal that the overpotential value of the MoS_2 electrode is about 160 mV, and that of the Pt is near zero, while the overpotential value of the bulk MoS_2 was much higher than the stated values.

The Tafel slope of the Pt catalyst is $\sim$35 mV dec^{-1} and for molybdenum quantum dots it is about $\sim$59 mV dec^{-1} which are comparatively lower value than that of the bulk sample with the value of $\sim$132 mV dec^{-1} (Fig. 11b and c).

This work idealizes MoS_2 quantum dots and their layering to increase the efficiency of this cost-efficient electrocatalyst and lower them into ultra-small sizes for profound results of hydrogen evolution (Fig. 11d and e).

3.3.1. Doped with carbonaceous materials. Carbon is considered an inert material in almost all electrochemical

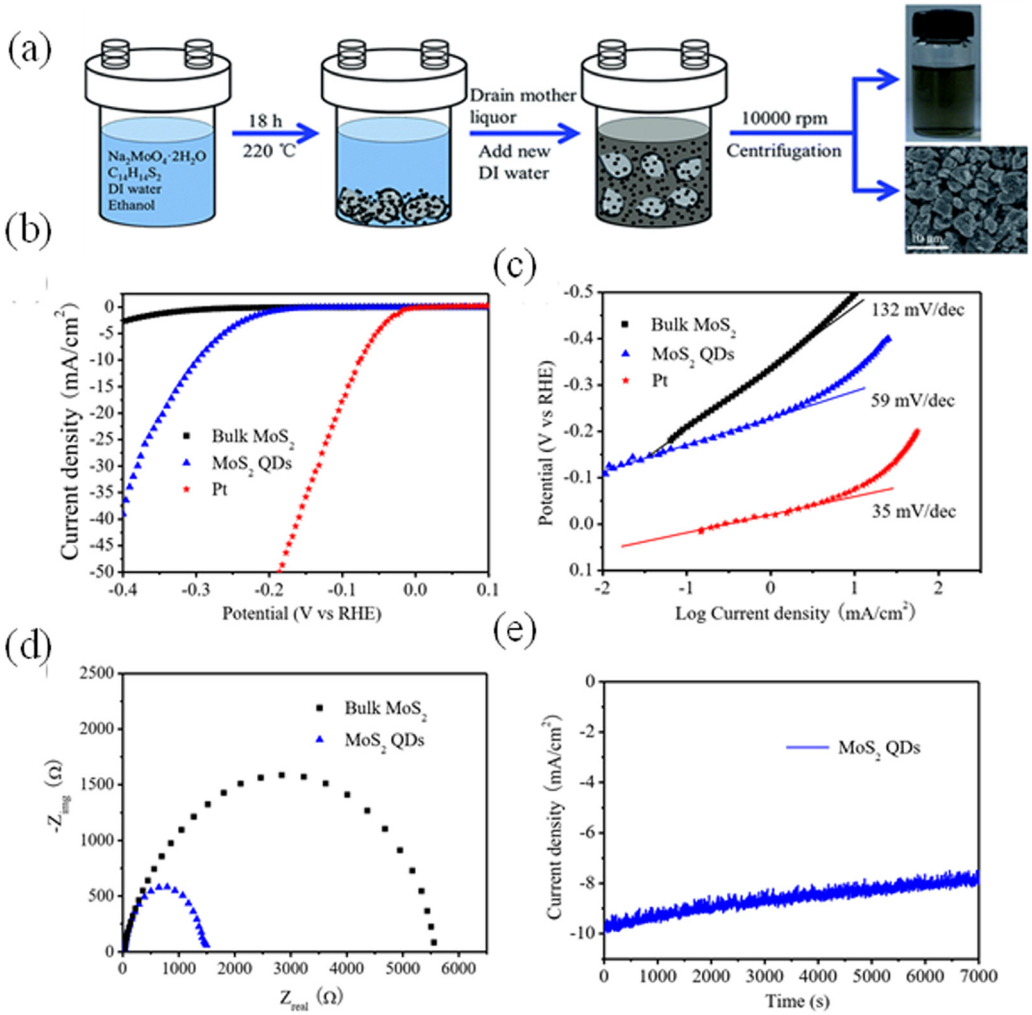

Fig. 11 (a) Synthesis methodology for the preparation of monolayer MoS_2. Electrochemical polarisation curve (b), Tafel slope (c), Nyquist plot (d) and stability study (e) of the monolayer MoS_2. Reproduced from ref. 114 (Copyrights 2022, Royal Society of Chemistry).

reactions, including the hydrogen evolution reaction as well. Doping of heteroatoms or several other transition metal atoms into the carbon structure helps in modifying the electronic properties of carbon and helps in the creation of more active sites for producing hydrogen.[115] Feng Li *et al.*, reported a facile sonication process for the synthesis of MoS_2 quantum dots decorated over RGO, for the electrocatalytic hydrogen evolution reaction (Fig. 12).[116]

The synthesized catalyst is known to have electro-conductive RGO, which can create freestanding, thin van der Waals heterostructures automatically. The synthetic nanocomposite showed enhanced HER activity with an onset potential of about −8 mV, a current density of 0.669 mA cm^{-2}, and a Tafel plot value measuring 63 mV dec^{-1}, showing better stability as well.

The composite is known to be highly active, durable, and considered a promising alternative material in place of noble metal catalysts used for HER.

Zhang *et al.* tailored an efficient route for the synthesis of cobalt phosphide (Co_2P) quantum dots incorporated with nitrogen, carbon over a carbon cloth was doped dually with phosphorous, and the reaction is carried out *in situ* by carbonization of cobalt ions, which is carefully induced to polyaniline and phytic acid macromolecule precursors.[117] Highly active electrochemical sites and charge transport are enabled with quite low resistance, which is primarily due to the cumulative effects of N, P dual-doped carbon frameworks and Co_2P quantum dots. Electrochemical studies reveal that the as-prepared catalyst is known to exhibit good electrochemical activity for efficient hydrogen production in both acidic and alkaline media. The acidic medium was found to be superior in activity to the alkaline one. The overpotential of the catalyst at a current density of 10 mA cm^{-2} is experimentally known to be 116 mV in the acidic medium and 129 mV in the alkaline medium, respectively. In comparison to the Tafel slope values for the catalyst, a smaller Tafel slope value of about 93 mV dec^{-1} was calculated for acidic electrolytes. Thus, the obtained catalyst Co_2P@NPC-800 works well in both acidic and alkaline electrolytic conditions and concluded that the catalytic performance is enhanced in an acidic medium than in an alkaline medium. Zonghua Pu *et al.*, in 2016, illustrated a one-step simple

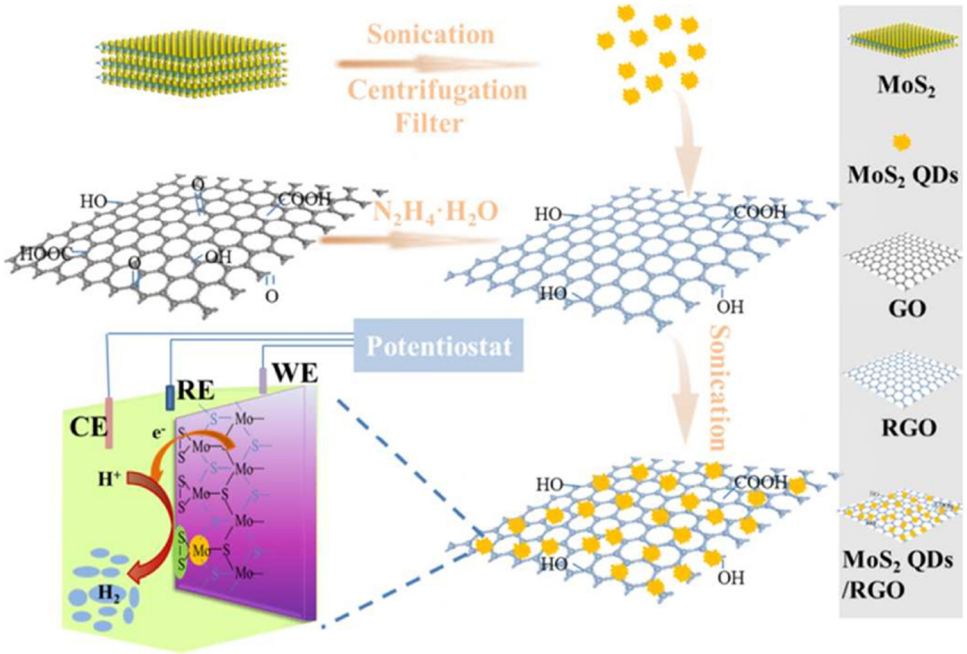

Fig. 12 Graphical depiction of the design and development of MoS_2 quantum dots on reduced graphene oxide catalyst. Reproduced from ref. 116 (Copyrights 2022, Royal Society of Chemistry).

methodology for the synthesis of MoP Nps@NC.[118] The synthesized catalyst is known to show good HER efficacy with an overpotential value of about 136 mV and 80 mV in 0.5 M H_2SO_4 and 1.0 M phosphate buffer solutions, respectively, when the current density is about 10 mA cm^{-2} (Fig. 13a–e).

3.3.2. Doped with metal-based materials. Shengjie *et al.* reported the facile synthesis of transition metal dichalcogenide quantum dots that were employed in the electrocatalytic production of hydrogen.[119]

MoS_2/WS_2 quantum dots could be prepared under simple experimental conditions such as ultra-sonication and solvothermal processes under mild temperature from the bulk MoS_2/WS_2. To measure the hydrogen evolution capacity of this material, a standard three-electrode was set up by employing 0.5 M sulphuric acid as the electrolyte, with a scan rate of about 5 mV s^{-1}. As it is known that bulk MoS_2 is associated with lower catalytic activity, as well as MoS_2/WS_2 when compiled to form a composite, the decrease in the catalytic activity was anticipated. After the solvothermal process, the as-prepared composite of MoS_2/WS_2 tends to show a lower onset overpotential $\approx$120 mV for the hydrogen evolution reaction.

This enhanced catalytic activity is specifically due to the MoS_2 quantum dots that are interspersed in MoS_2 nanosheets, which are believed to have enriched defects. As such, the materials have more active edge sites for hydrogen evolution. The random layering of the nanosheets onto the surface of the glassy carbon electrode is used as a key for the efficient electron transfer between the underlying electrode and the active edge sites. The work reported that the combination of sonication and the solvothermal process can be a perspective synthesis method for preparing effective TMD material for HER since the as-prepared composite is said to possess better catalytic activity than the individual WS_2 and MoS_2.

Yu *et al.*,[120] fabricated a facile synthesis method for the self-assembly of Au/MoS_2, which is a core-satellite hybrid material, efficiently utilized as a catalyst for electro-catalytic Hydrogen Evolution Reaction (HER). In this work, the performance of the catalyst was in comparison with that of Au nanoparticles, 20% Pt/C and MoS_2 quantum dots. The presence of a higher number of edge sites on MoS_2 and the aggregated high conductance of the Au nanoparticles was attributed to the better HER performance of the hybrid material. On the basis of the experiments, it was studied that the hybrid Au/MoS_2 quantum dots will require overpotential values of about 206, 146, and 112 mV to drive current density values of 50, 20, and 10 mA cm^{-1}, respectively (Fig. 14a–d).

Li *et al.*,[121] developed a new novel ruthenium nanoparticle that is loaded with carbon quantum dots used to be a competent electrocatalyst in the HER. The electrochemical studies of this material showed that under extreme conditions of alkalinity, the as-synthesized material showed up outstanding catalytic effects with an overpotential of about 10 mV and has good durability. The value of the Tafel slope for this material was 47 mV dec^{-1} (Fig. 15). Dang *et al.*,[122] reported a novel work by obtaining Rh–Si composites, wherein the Rh nanocrystals are made to grow on the surface of the silicon quantum dots which is aided by the Si–H bonds (Fig. 16).

Based on electrochemical studies at optimal conditions, the as-prepared material shows a low Tafel slope value of 26 mV dec^{-1} (Fig. 17a–d), as it is found to be stable for a longer time. The efficiency provided by this material is shown in spite of lower amounts of noble metal usage than usually employed in 20 wt% Pt/C, substantiating novelty.

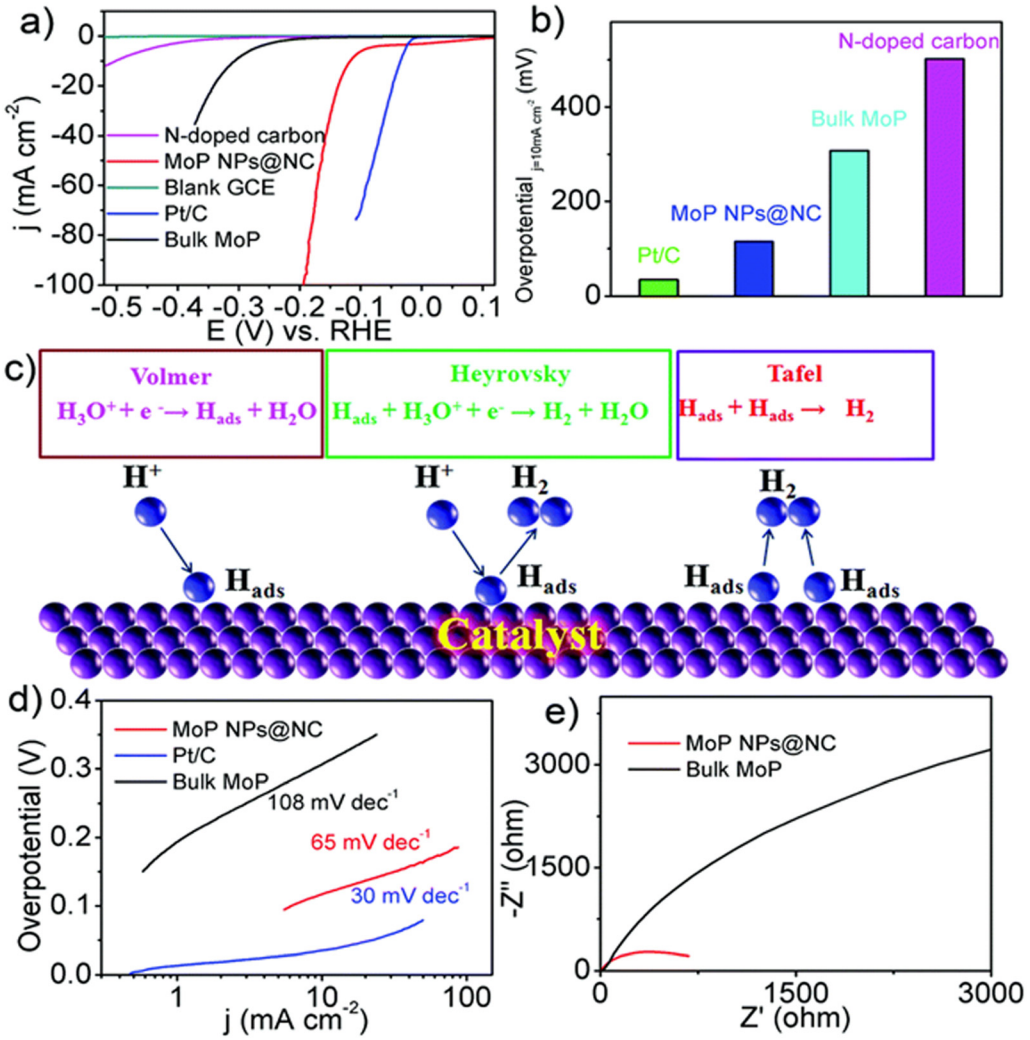

Fig. 13 Polarisation curve (a), the overpotential values at 10 mA cm^{-2} (b), the HER (c), Tafel plot (d) and Nyquist plot (e). Reproduced from ref. 118 (Copyrights 2022, Royal Society of Chemistry).

3.3.3. Variation in the TMQDs with typical reaction conditions. Metal sulphide composites are considered comparatively with other composites because they have good electrochemical properties for HER catalysis. The efficacy of metal sulphides is greatly limited due to the finite number of active sites and low intrinsic activity. There are certain ways to optimally customize the multifunctional electrochemical properties. Initially, it is important to elevate the number of active sites present per unit area. In general, it is known that the efficiency of an electrocatalyst is largely correlated with the dimension it possesses. To be more precise, we know that controlling the catalyst size within nanoscale ranges will enhance the active sites and increase the contact area between the electrolyte and the catalyst.

Thus, this curtails the pathway available for electron transfer. Such results are possible only when the material is in nanoscale and not in bulk scales.[123] Either way of enhancing the efficiency of electrocatalyst is to electronically modify the structural properties of the electrocatalyst to increase the activity of each active site.[124] An additional method to overcome this issue is to make available higher surface area in materials by proper nanoscale designing, for example, mesopores, nanoparticles, nanosheets and nanowires.[125]

Zhang *et al.* tailored an efficient synthesis method for the preparation of cobalt-doped Mo, Z-ZIF derived Co_9S_8 quantum dots wherein the MoS_2 was embarked in the nanoflake arrays of carbon, which was doped with 3D nitrogen, and the system was supported on carbon nanofibers (Co_9S_8-MoS_2/N-CNAs@CNFs).[126] This material is said to have a unique 3D structure owing to its trifunctionality for OER and HER applications. Electrocatalytic studies revealed that Co_9S_8-MoS_2/N-CNAs@CNFs are known to have a current density with the value of 10 mA cm^{-2} and possess an overpotential of 163 mV for hydrogen evolution reactions. This scale value is typically an efficient outcome when compared with the traditional MOF-derived transition metal sulphide catalysts (Fig. 18a and b). Huo *et al.* synthesized a novel well-defined heterojunction of molybdenum carbide-tungsten carbide quantum dots, which were 0-dimensional and 2-dimensional decorated

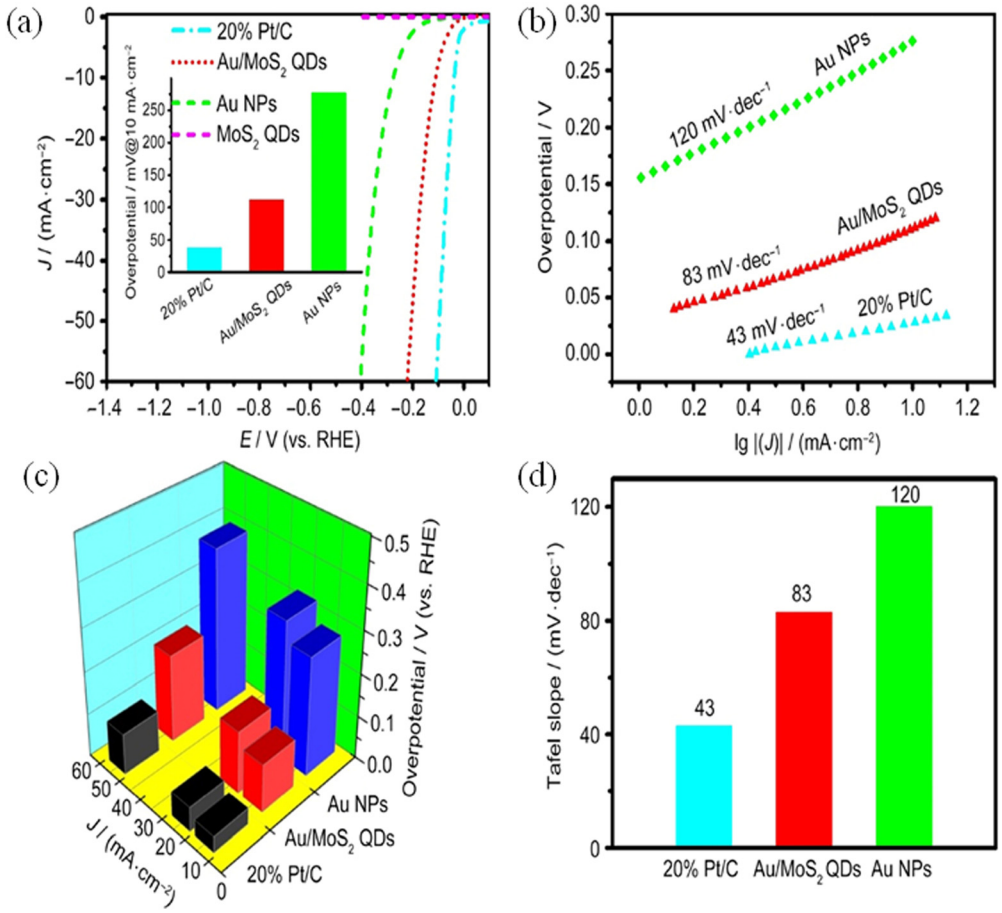

Fig. 14 Electrocatalytic performance with polarisation curve (a), Tafel plot (b), overpotential at different current densities and composite (c) and histogram for Tafel slope (d). Reproduced from ref. 120 (Copyrights 2022, Springer Nature).

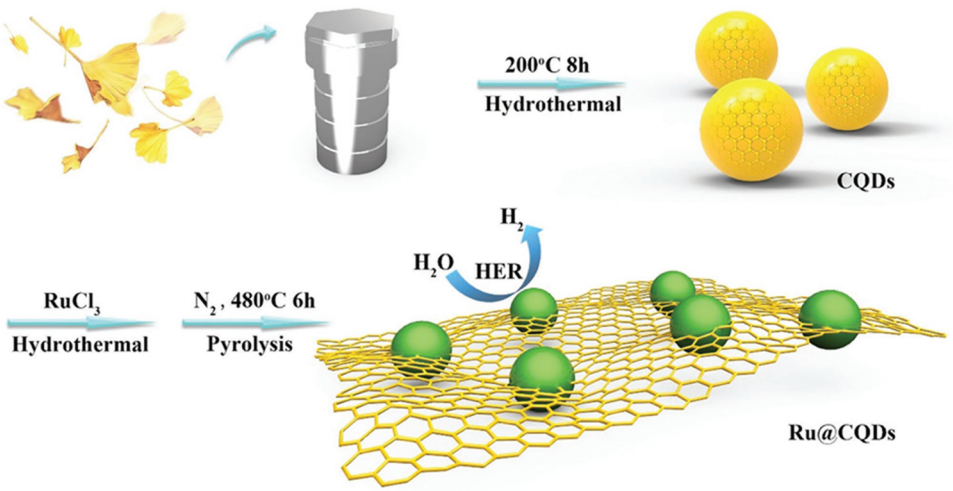

Fig. 15 Pictorial depiction of the synthesis and HER activity of Ru@CQDs480 electrocatalyst. Reproduced from ref. 121 (Copyrights 2018, John Wiley & Sons).

over N-doped graphene nanosheets through a nano-casting method using a standard template KIT 6/graphene.[127] Under acidic conditions, $(Mo_2C)_{0.24}$-$(WC)_{0.52}$-QDs/NG, $(Mo_2C)_{0.41}$-$(WC)_{0.18}$-QDs/NG, and $(Mo_2C)_{0.34}$-$(WC)_{0.32}$-QDs/NG needed an overpotential value of about 100, 100, 119, 146, and 175 mV, respectively (Fig. 19a and b).

These overpotential values are lower than that of WC-QDs/NG (175 mV and 204 mV) and Mo_2C-QDs/NG (146 and 181 mV).

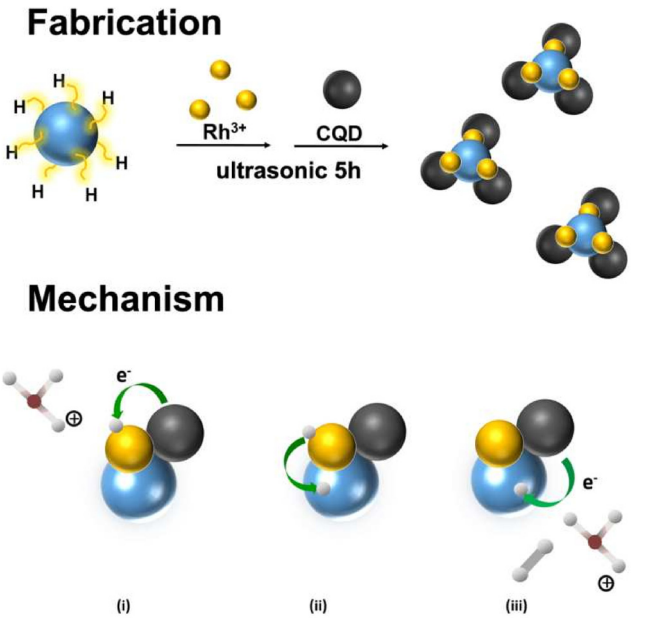

Fig. 16 Fabrication of Rh/SiQD/CQD nanocomposites and mechanism of reaction. Reproduced from ref. 122 (Copyrights 2022, Elsevier B.V.).

The greater efficiency of this catalyst could be attributed to the incorporation of MoC-WC, which has led to the redistribution of electrons in the valence bands and boosted conductivity as observed with the Tafel values (Fig. 19c and d). With all this effectiveness, this material has proved to be an excellent catalyst to produce hydrogen from water.

Ye *et al.* reported Pt(III) quantum dots on flower-like α-Fe_2O_3 thin film nanosheets. The material showed excellent water splitting activity due to the bifunctional catalytic activity, which is attributed to the quantum size effect and many active sites.[128] The active sites could offer greater efficiency with a lower overpotential of 90 mV and a Tafel slope of 49.6 mV dec^{-1} and the overall water splitting was obtained at a low voltage of 1.51 V in alkaline KOH conditions, which is remarkable.

The close contact of Pt QDs with the nanosheets reinforced the quantum size effect, thus leading to the synergetic effect and the enhancement of the electron transfer rate. Das *et al.* incorporated *N*,*N*′-dibenzoyl-L-cystine (DBC) hydrogels into the polymer matrix of polyaniline(PANI) synthesizing an aerogel DBC-MoS2-PANI with 2 different composition ratios and acquired the lowest overpotential of 196 mV and a Tafel slope of 58 mV dec^{-1} (Fig. 20).[129] The surface modification results in higher efficiency along with the photo-response property of the material. Liu *et al.*[130] in 2022 studied the evolution of surface-active groups of MXene Quantum Dots composed of Ti_2CT_x, wherein Cl – groups are continuously replaced by O-terminated groups, while the reaction takes place in the cathode. The material was found to have good electrocatalytic efficiency towards HER with a lower overpotential value of about 175 mV owning to a current density of 10 mA cm^{-1} in an electrolytic solution of 1 M aq. KOH. For this value of current density, the electrocatalyst was found to be highly stable over a period of 165 h.

Dinda *et al.*, amorphized MoS_2 QDs *via* a simple chemical reaction, obtaining a QD of ~4 nm.[131] The onset potential and superior electrocatalytic activity of the material are ascribed to

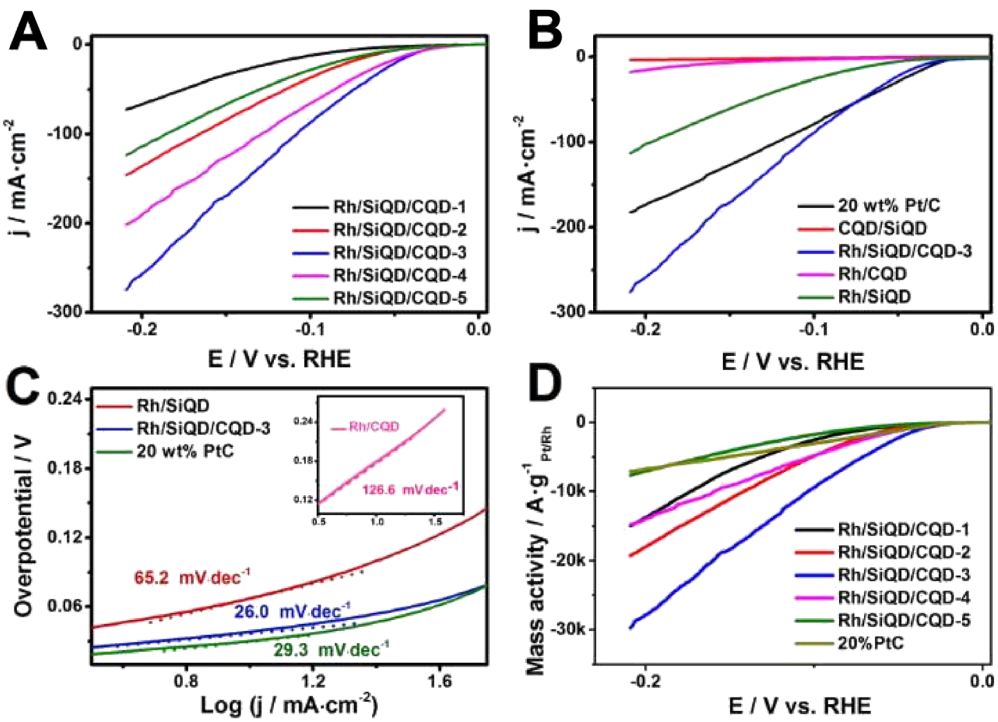

Fig. 17 LSV curves (a and b), Tafel plot (c) and mass activity (d) of the nanocomposite. Reproduced from ref. 122 (Copyrights 2022, Elsevier B.V.).

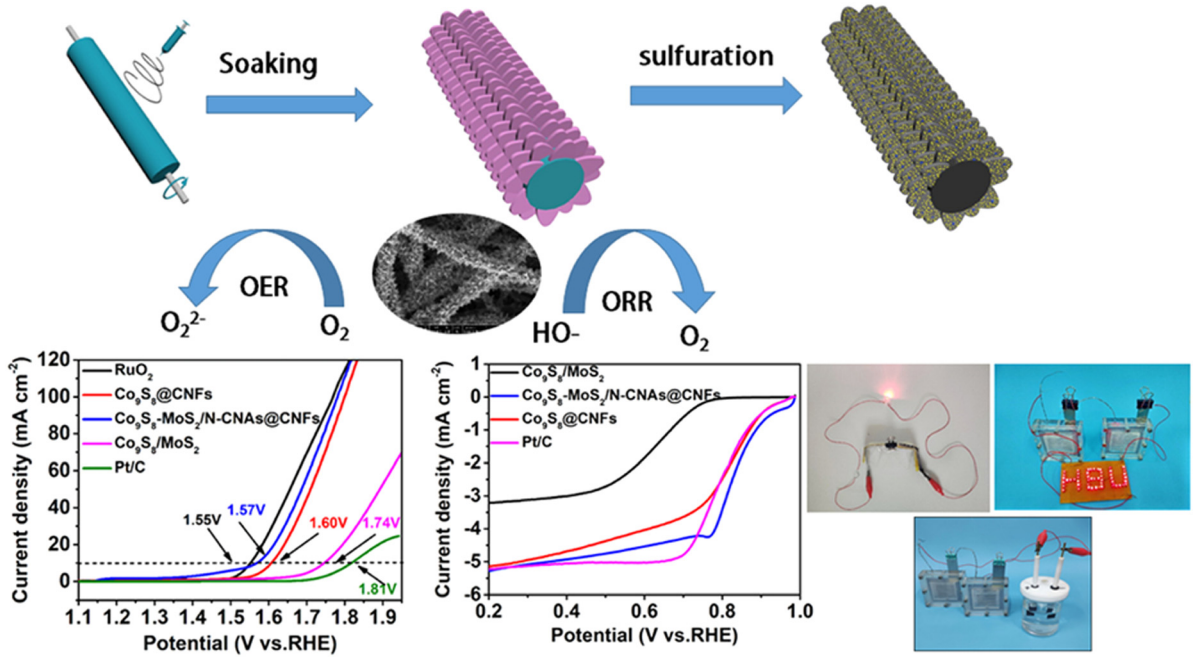

Fig. 18 Schematic representation of the preparatory scheme of Co_9S_8-MoS_2/NCNAs@CNFs (a). Polarisation curve with the pictorial representation of the circuit (b). Reproduced from ref. 126 (Copyright 2022, American Chemical Society).

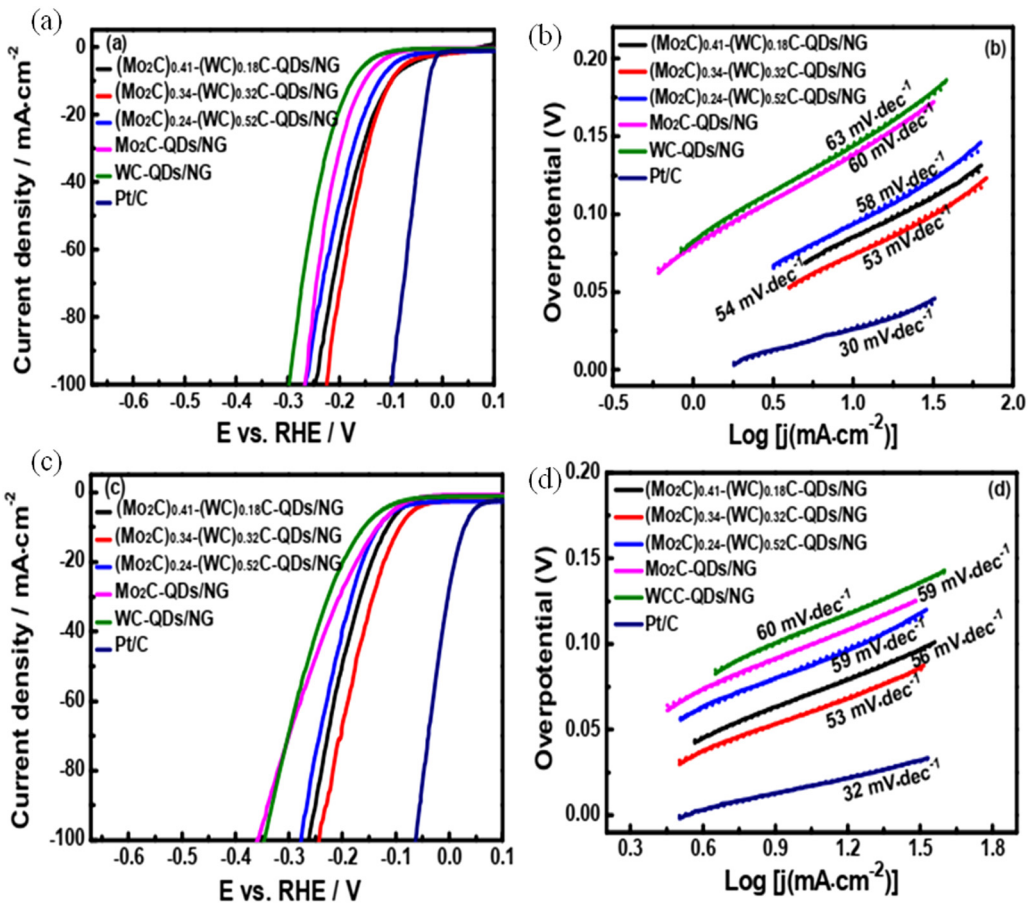

Fig. 19 The polarisation curves (a and c) and the Tafel slope (b and d) for the studied samples. Reproduced from ref. 127 (Copyrights 2017, Royal Society of Chemistry).

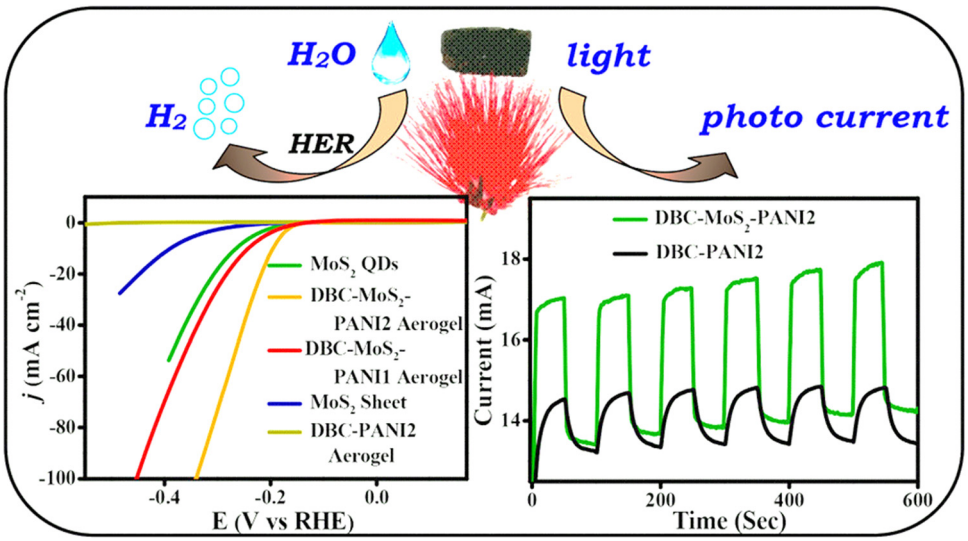

Fig. 20 The overall representation of the hydrogen evolution along with the polarisation curve and photo response property of DBC-MoS_2-PANI and its composites. Reproduced from ref. 129 (Copyright 2018, American Chemical Society).

the unsaturated sulphur ligands and a higher number of active edge sites to an overpotential of 65 mV and the Tafel slope value of 73.9 mV decade. The amorphization could clearly be observed in the SAED pattern and blue shift in the peaks of the Raman analysis. The unsaturated sulphur ligands were confirmed with the XPS analysis (Fig. 21).

This material showed a pathway as an efficient electrocatalyst for energy production due to its quantum confinement and more active unsaturated sulphur ligands. Currently, there are several reports with quantum dots as electrocatalysts for efficient HER, and the current review comprises the study of the recent advances, efficiency, as well as advantages of these TMQDs composites as electrocatalysts for HER; Table 2 represents the few recent reports of QDs based electrocatalysts utilized in HER.

3.4. Major challenges and impact of TMQDs as electrocatalysts

Electrocatalysts are indispensable for lowering the kinetic barrier for HER. The specific challenge faced is that utilisation

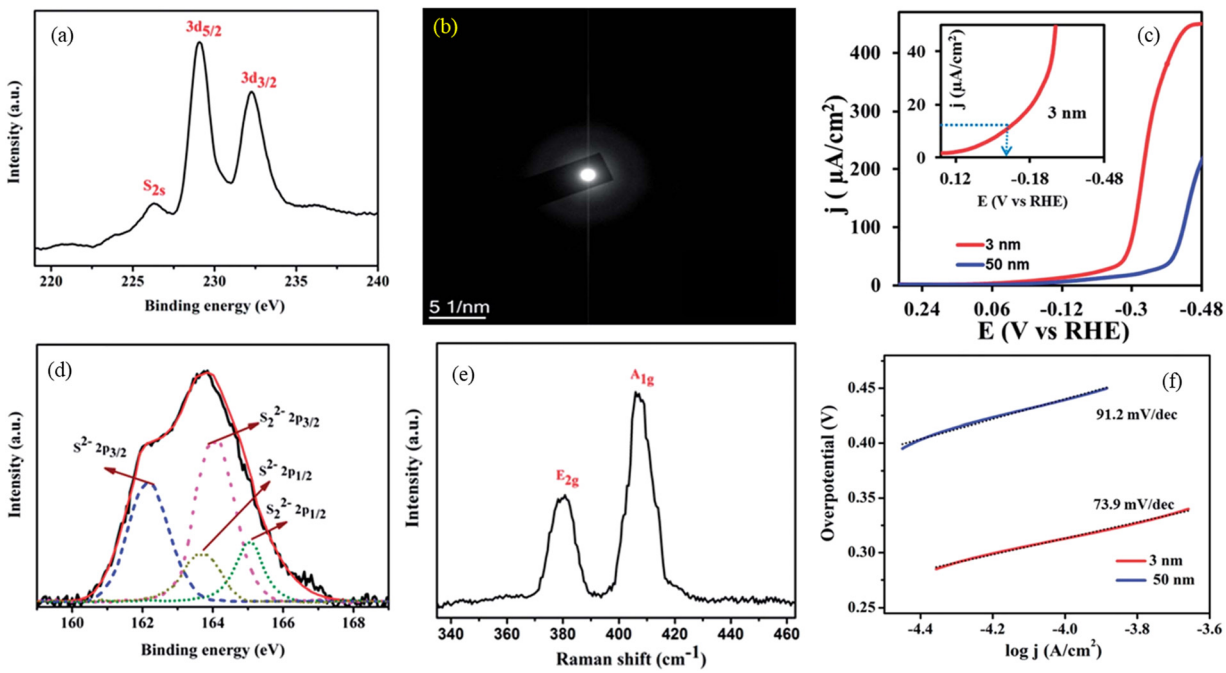

Fig. 21 S 3d and S 2s XPS (a), SAED pattern (c) for the catalyst with polarisation curves (d) S 2p XPS, (e) Raman spectra (f) the Tafel slope for the studied samples. Reproduced from ref. 131 (Copyrights 2017, Royal Society of Chemistry).

Table 2 Recent developed QDs as an electrocatalyst for HER

Sl. no.	Material	Synthesis methods	Electrolyte	Mechanistic pathway followed	Overpotential at 10 mA cm^{-2}	Tafel slope (mV dec^{-1})	Ref.
1.	MoS_2 quantum dots decorated RGO	Facile sonication	0.5 M H_2SO_4	Heyrovsky-Volmer	64 mV	63	132
2.	Monolayer MoS_2 quantum dots	Facile hydrothermal	0.5 M H_2SO_4	—	160 mV	59	133
3.	Solution-processed hybrid graphene flake/2H-MoS_2 quantum dot heterostructures	One-step solvothermal	0.5 M H_2SO_4	Heyrovsky–Volmer	136 mV	~82	134
4.	Two-dimensional dual-carbon-coupled defective nickel quantum dots	one-pot thermal treatment	1 M KOH	Heyrovsky–Volmer	133 mV	65	135
5.	SnS_2 quantum dots growth on MoS_2	Facile hydrothermal	0.5 M H_2SO_4	Heyrovsky–Volmer	240 mV	65	136
6.	MoS_2 quantum dots and pore-rich monolayer MoS_2	Gas phase etching	0.5 M H_2SO_4	Volmer	241 mV	163	137
7.	VSe_2 quantum dots on carbon cloth	Tip sonication	0.5 M H_2SO_4	—	0.40 V	80	138
8.	Pt QDs@Nb_2CT_x nanowire	Solution-based	1 M H_2SO_4	Heyrovsky–Volmer	33.3 mV	29	139
9.	Pt QDs@Nb_2CT_x nanowire	Solution-based	1 M KOH	Tafel–Volmer	61.5 mV	58	139
10.	Quasi zero-dimensional MoS_2 quantum dots decorated 2D $Ti_3C_2T_x$ MXene	Facile hydrothermal	0.5 M H_2SO_4	Heyrovsky–Volmer	220 mV	72	140
11.	Two-dimensional PtS_2 quantum dots/TiC	Thermal treatment	0.5 M H_2SO_4	Heyrovsky–Volmer	55 mV	60	141
12.	$Ni_3Sn_2S_2$@Ni_3S_2 NF	Chemical vapor deposition	1.0 M KOH	Heyrovsky–Volmer	53.2 mV	73.2	142
13.	Ruthenium quantum dots supported on carbon nanofibers	Simple adsorption and pyrolysis	1.0 M KOH	—	20 mV	31	143
14.	MoS_2 quantum dots@TiO_2 nanotube arrays	Electrochemical exfoliation with electrophoretic deposition (EFED)	0.5 M H_2SO_4	—	76 mV	93	144
15.	$CoSe_2$ QDs with $MoSe_2$ nanosheets heterostructures	Hydrothermal	1.0 M KOH	Heyrovsky–Volmer	218 mV	76	145
16.	PbTe quantum dots with amorphous MoS_x/TiO_2 nanotube arrays	Successive ionic layer adsorption and reaction (SILAR) and electrodeposition	0.5 M H_2SO_4	Heyrovsky–Volmer	~300 mV	42	146
17.	Mo_2C quantum dots embedded chitosan-derived nitrogen-doped carbon	Scalable solid-state reaction	1.0 M KOH	Heyrovsky–Volmer	160 mV	55	147
18.	α-MoC_{1-x} quantum dots encapsulated in nitrogen-doped carbon	Solidoid nitridation reduction	1.0 M KOH	Heyrovsky–Volmer	118 mV	84	148
19.	MoS_2 QDs@Graphene	lyophilization	0.5 M H_2SO_4	Heyrovsky–Volmer	140 mV	68	149
20.	Three-dimensional (3D) MoS_2 quantum dots (MoS_2QD) aaerogel	Hydrothermal	0.5 M H_2SO_4	Heyrovsk–Volmer	53 mV	41	150

of QDs as a single-component catalyst is not practically stable and can only be used as an efficient catalyst when designed as a composite. The stability of the electrocatalyst and agglomeration of the material are the major challenges with QDs. Thus, it is important to design and develop QDs, which can stand alone and act as an electrocatalyst that possesses greater stability. The issue of agglomeration can be addressed by storing it in a conducive atmosphere, such as storing it at low temperatures, *etc.*

3.5. Future perspective

Even though breakthroughs are frequently based on a rationale that includes the results of numerous studies in the field, the basic attributes of favourable electrocatalysts can be explained simply as in the electrochemical reactions. With reference to the work done earlier, there are reports that showed hybrid structures' effect of the electrocatalyst with positive outcomes. It can be assumed that there will be fewer obstacles in scaling up the electrocatalyst for HER application if we lower the cost of the catalyst production by lowering the economic scales. when the HER application is synergistically utilized with industry, the burden on fossil fuel consumption will be reduced, thereby reducing the carbon footprint, with an efficient and stable electrocatalyst. Along with the experimental studies, a better understanding of the mechanism, and designing a catalyst, there is a great need for computational studies to provide the direction of the reaction pathway. With this, there is a greater need for future research to focus on finding, predicting, and screening the TMQDs for high-performance output, which can be further combined with machine learning and can be utilized effectively for scale-up. Standardization of measurements, such as electrode surface area, electrode configuration, catalyst activity, mass loading, and other calculation methods, is essential to accurately and fairly understand the performances of the reported works. Furthermore, in order to bridge the gap between the research lab and the market, the researchers should aim to achieve good experiment results that are practically applicable in real time. As a result, electrochemical measurements are highly recommended in the current situation to further enhance hydrogen evolution.

4. Conclusions

The electrochemical HER is growing as one of the prominent replacements for energy generation in sustainable energy goals

and making the hydrogen economy the reality for everyday use. For this, a cost-effective catalyst, efficient, and has higher activity, stability, and durability for the long term is essential to realise hydrogen generation economically. In this review, we briefed the current upliftment of the vision of QDs as an electrocatalyst for HER application, which emphasizes the electrochemical performance along with the mechanism related to its activity. To generalize, the good catalytic performance of the QDs in HER application is accredited to the greater intrinsic activity, increased number of active sites, a higher number of atoms exposed, or increased charge transfer and mass transfer process. All together were finely spindled to the tuning of the surface, the collaborative effect between the materials, structure modulation, and many more factors. Despite all these achievements in the QDs as electrocatalysts in HER, hydrogen production is a few steps away from practical application. The electrocatalyst having a greater surface area and a large number of active atoms is efficient and effective for hydrogen production. Along with this, a few basic and real-world issues should be addressed completely to equip the QDs as electrocatalysts. Still, there is a need to understand the fundamentals and mechanisms of HER. Along with shifting from the expensive Pt-electrocatalysts with lower stability until it is made of a composite with carbon for support, which increases the operation cost higher, to less expensive materials with higher stability are rather mandatory than left out as a choice. The prospects depend on finding a solution to the pressing issues, which range from catalyst design to reaction kinetics and mechanism.

Importantly, the vast bulk TMQDs can demonstrate excellent HER in the acidic medium and their performance in alkaline or neutral electrolytes are generally poor or has not been fully reviewed. Improving the electrocatalytic activity of TMQDs and expounding their reaction mechanisms in different electrolytes are essential for the widespread application of these materials. Attempts should be made to implement strategies that reduce the energy barriers for water dissociation on catalyst surfaces in alkaline media. For instance, in recent years, with the incorporation of the first row of transition metals (Ni, Co, and Fe) or the doping of rare metals (Ru), TMQDs have shown superb HER performances in the alkaline environment.

Author contributions

Brahmari Honnappa: investigation, writing – review and editing, writing – original draft. Sathya Mohan: writing – review and editing. Ashil Augustin: writing – review and editing. Mariyappan Shanmugam: writing – review and editing. Prince J. J. Sagayaraj: writing – editing. Chitiphon Chuaicham: writing – review and editing. Saravanan Rajendran-review and editing. Tuan K. A. Hoang – review and editing. Keiko Sasaki: writing – review and editing. Karthikeyan Sekar: writing – review and editing, investigation.

Conflicts of interest

There are no conflicts to declare.

Acknowledgements

S. K. acknowledges the Royal Society-Newton International Fellowship Alumni follow-on funding support AL/211016, UK and Department of Chemistry at the SRM Institute of Science and Technology, India.

References

1 E. Guilyardi, L. Lescarmontier, R. Matthews, S. P. Point, A. B. Rumjaun, J. Schlüpmann and D. Wilgenbus, 2018.
2 B. JO'M, *Int. J. Hydrogen Energy*, 2002, **27**, 731–740.
3 G. Marbán and T. Valdés-Solís, *Int. J. Hydrogen Energy*, 2007, **32**, 1625–1637.
4 L. Barreto, A. Makihira and K. Riahi, *Int. J. Hydrogen Energy*, 2003, **28**, 267–284.
5 Z.-Y. Yu, Y. Duan, X.-Y. Feng, X. Yu, M.-R. Gao and S.-H. Yu, *Adv. Mater.*, 2021, **33**, 2007100.
6 B. Ma, H. Zhao, T. Li, Q. Liu, Y. Luo, C. Li, S. Lu, A. M. Asiri, D. Ma and X. Sun, *Nano Res.*, 2021, **14**, 555–569.
7 Y. Wang, B. Liu, Y. Liu, C. Song, W. Wang, W. Li, Q. Feng and Y. Lei, *Chem. Commun.*, 2020, **56**, 14019–14022.
8 Y. Jiao, Y. Zheng, M. Jaroniec and S. Z. Qiao, *Chem. Soc. Rev.*, 2015, **44**, 2060–2086.
9 L. Wang, Y. Zhu, Y. Wen, S. Li, C. Cui, F. Ni, Y. Liu, H. Lin, Y. Li and H. Peng, *Angew. Chem.*, 2021, **133**, 10671–10676.
10 I. Roger, M. A. Shipman and M. D. Symes, *Nat. Rev. Chem.*, 2017, **1**, 1–13.
11 J. Liu, T. He, Q. Wang, Z. Zhou, Y. Zhang, H. Wu, Q. Li, J. Zheng, Z. Sun and Y. Lei, *J. Mater. Chem. A*, 2019, **7**, 12451–12456.
12 E. Liu, J. Li, L. Jiao, H. T. T. Doan, Z. Liu, Z. Zhao, Y. Huang, K. Abraham, S. Mukerjee and Q. Jia, *J. Am. Chem. Soc.*, 2019, **141**, 3232–3239.
13 G. Zhao, J. Chen, W. Sun and H. Pan, *Adv. Funct. Mater.*, 2021, **31**, 2010633.
14 Y. Zhou, Z. Xie, J. Jiang, J. Wang, X. Song, Q. He, W. Ding and Z. Wei, *Nat. Catal.*, 2020, **3**, 454–462.
15 X. X. Wang, M. T. Swihart and G. Wu, *Nat. Catal.*, 2019, **2**, 578–589.
16 M. Yang, C. H. Zhang, N. W. Li, D. Luan, L. Yu and X. W. Lou, *Adv. Sci.*, 2022, **9**, 2105135.
17 G. Zhan, P. Li and H. C. Zeng, *Adv. Mater.*, 2018, **30**, 1802094.
18 Y. Yu, Y. Shi and B. Zhang, *Acc. Chem. Res.*, 2018, **51**, 1711–1721.
19 J. Liu, D. Zhu, C. Guo, A. Vasileff and S. Z. Qiao, *Adv. Energy Mater.*, 2017, **7**, 1700518.
20 J. Lee, S. M. Kim and I. S. Lee, *Nano Today*, 2014, **9**, 631–667.
21 J. Park, T. Kwon, J. Kim, H. Jin, H. Y. Kim, B. Kim, S. H. Joo and K. Lee, *Chem. Soc. Rev.*, 2018, **47**, 8173–8202.
22 B. W. Xue, C. H. Zhang, Y. Z. Wang, W. W. Xie, N.-W. Li and L. Yu, *Nanoscale Adv.*, 2020, **2**, 5555–5566.
23 R. E. Blankenship, D. M. Tiede, J. Barber, G. W. Brudvig, G. Fleming, M. Ghirardi, M. Gunner, W. Junge, D. M. Kramer and A. Melis, *Science*, 2011, **332**, 805–809.

24 H. Schafer, D. Chevrier, K. Kuepper, P. Zhang, J. Wollschlaeger, D. Daum and M. Steinhart, *Energy Environ. Sci.*, 2016, **9**, 2609–2622.
25 J. Zhu, L. Hu, P. Zhao, L. Y. S. Lee and K.-Y. Wong, *Chem. Rev.*, 2020, **120**, 851–918.
26 P. C. K. Vesborg, B. Seger and I. Chorkendorff, *J. Phys. Chem. Lett.*, 2015, **6**, 951–957.
27 W. Vielstich, A. Lamm and H. Gasteiger, 2003.
28 N. Dubouis and A. Grimaud, *Chem. Sci.*, 2019, **10**, 9165–9181.
29 M. J. T. C. van der Niet, N. Garcia-Araez, J. Hernández, J. M. Feliu and M. T. M. Koper, *Catal. Today*, 2013, **202**, 105–113.
30 I. T. McCrum and M. J. Janik, *J. Phys. Chem. C*, 2016, **120**, 457–471.
31 X. Chen, I. T. McCrum, K. A. Schwarz, M. J. Janik and M. T. M. Koper, *Angew. Chem., Int. Ed.*, 2017, **56**, 15025–15029.
32 J. K. Nørskov, T. Bligaard, A. Logadottir, J. Kitchin, J. G. Chen, S. Pandelov and U. Stimming, *J. Electrochem. Soc.*, 2005, **152**, J23.
33 S. Trasatti, *J. Electroanal. Chem. Interfacial Electrochem.*, 1972, **39**, 163–184.
34 J. K. Nørskov, T. Bligaard, A. Logadottir, J. R. Kitchin, J. G. Chen, S. Pandelov and U. Stimming, *J. Electrochem. Soc.*, 2005, **152**, J23.
35 A. R. Zeradjanin, J.-P. Grote, G. Polymeros and K. J. J. Mayrhofer, *Electroanalysis*, 2016, **28**, 2256–2269.
36 T. F. Jaramillo, K. P. Jørgensen, J. Bonde, J. H. Nielsen, S. Horch and I. Chorkendorff, *Science*, 2007, **317**, 100–102.
37 Y. Li, H. Wang, L. Xie, Y. Liang, G. Hong and H. Dai, *J. Am. Chem. Soc.*, 2011, **133**, 7296–7299.
38 L. Liao, J. Zhu, X. Bian, L. Zhu, M. D. Scanlon, H. H. Girault and B. Liu, *Adv. Funct. Mater.*, 2013, **23**, 5326–5333.
39 E. Skúlason, V. Tripkovic, M. E. Björketun, S. Gudmundsdóttir, G. Karlberg, J. Rossmeisl, T. Bligaard, H. Jónsson and J. K. Nørskov, *J. Phys. Chem. C*, 2010, **114**, 18182–18197.
40 D. M. Santos, C. A. Sequeira and J. L. Figueiredo, *Química Nova*, 2013, **36**, 1176–1193.
41 T. J. Schmidt, V. Stamenkovic, J. P. N. Ross and N. M. Markovic, *Phys. Chem. Chem. Phys.*, 2003, **5**, 400–406.
42 N. Mahmood, Y. Yao, J.-W. Zhang, L. Pan, X. Zhang and J.-J. Zou, *Adv. Sci.*, 2018, **5**, 1700464.
43 M. Lao, K. Rui, G. Zhao, P. Cui, X. Zheng, S. X. Dou and W. Sun, *Angew. Chem., Int. Ed.*, 2019, **58**, 5432–5437.
44 Q. Xu, Y. Liu, H. Jiang, Y. Hu, H. Liu and C. Li, *Adv. Energy Mater.*, 2019, **9**, 1802553.
45 D. Strmcnik, P. P. Lopes, B. Genorio, V. R. Stamenkovic and N. M. Markovic, *Nano Energy*, 2016, **29**, 29–36.
46 M. M. Jakšić, *Int. J. Hydrogen Energy*, 1987, **12**, 727–752.
47 B. E. Conway and G. Jerkiewicz, *Solid State Ionics*, 2002, **150**, 93–103.
48 J. Greeley, T. F. Jaramillo, J. Bonde, I. B. Chorkendorff and J. K. Nørskov, *Nat. Mater.*, 2006, **5**, 909–913.
49 Z. Zeng, K.-C. Chang, J. Kubal, N. M. Markovic and J. Greeley, *Nat. Energy*, 2017, **2**, 17070.
50 M. Favaro, C. Valero-Vidal, J. Eichhorn, F. M. Toma, P. N. Ross, J. Yano, Z. Liu and E. J. Crumlin, *J. Mater. Chem. A*, 2017, **5**, 11634–11643.
51 B. E. Conway and L. Bai, *J. Electroanal. Chem. Interfacial Electrochem.*, 1986, **198**, 149–175.
52 B. E. Conway and G. Jerkiewicz, *Electrochim. Acta*, 2000, **45**, 4075–4083.
53 J. Wei, M. Zhou, A. Long, Y. Xue, H. Liao, C. Wei and Z. J. Xu, *Nano-Micro Lett.*, 2018, **10**, 75.
54 Y. Zheng, Y. Jiao, A. Vasileff and S. Z. Qiao, *Angew. Chem., Int. Ed.*, 2018, **57**, 7568–7579.
55 H. Fan, H. Yu, Y. Zhang, Y. Zheng, Y. Luo, Z. Dai, B. Li, Y. Zong and Q. Yan, *Angew. Chem., Int. Ed.*, 2017, **56**, 12566–12570.
56 H. Cheng, Y.-Z. Su, P.-Y. Kuang, G.-F. Chen and Z.-Q. Liu, *J. Mater. Chem. A*, 2015, **3**, 19314–19321.
57 L. Jin, H. Zhao, Z. M. Wang and F. Rosei, *Adv. Energy Mater.*, 2021, **11**, 2003233.
58 D. Kandi, S. Martha and K. M. Parida, *Int. J. Hydrogen Energy*, 2017, **42**, 9467–9481.
59 X. B. Li, C. H. Tung and L. Z. Wu, *Angew. Chem.*, 2019, **131**, 10918–10925.
60 M. Pohanka, *Mini Rev. Med. Chem.*, 2017, **17**, 650–656.
61 Y. Zhang, Y. Liu, C. Li, X. Chen and Q. Wang, *J. Phys. Chem. C*, 2014, **118**, 4918–4923.
62 W. C. Chan and S. Nie, *Science*, 1998, **281**, 2016–2018.
63 M. Bruchez Jr, M. Moronne, P. Gin, S. Weiss and A. P. Alivisatos, *Science*, 1998, **281**, 2013–2016.
64 A. S. Rasal, S. Yadav, A. Yadav, A. A. Kashale, S. T. Manjunatha, A. Altaee and J.-Y. Chang, *ACS Appl. Nano Mater.*, 2021, **4**, 6515–6541.
65 R. J. Warburton, *Contemp. Phys.*, 2002, **43**, 351–364.
66 H.-L. Wu, X.-B. Li, C.-H. Tung and L.-Z. Wu, *Adv. Mater.*, 2019, **31**, 1900709.
67 Q. Wu, X. Gong, D. Zhao, Y. B. Zhao, F. Cao, H. Wang, S. Wang, J. Zhang, R. Quintero-Bermudez and E. H. Sargent, *Adv. Mater.*, 2022, **34**, 2108150.
68 S. Anantharaj, M. O. Valappil, K. Karthick, V. K. Pillai, S. Alwarappan and S. Kundu, *Catal. Sci. Technol.*, 2019, **9**, 223–231.
69 R. Han, Q. Zhao, A. Hazarika, J. Li, H. Cai, J. Ni and J. Zhang, *ACS Appl. Mater. Interfaces*, 2022, **14**(3), 4061–4070.
70 V. Balakumar, M. Ramalingam, K. Sekar, C. Chuaicham and K. Sasaki, *Chem. Eng. J.*, 2021, **426**, 131739.
71 W. Wang and S. A. Asher, *J. Am. Chem. Soc.*, 2001, **123**, 12528–12535.
72 C. W. Wang, C. Orrison and D. H. Son, *Bull. Korean Chem. Soc.*, 2022, **43**, 492.
73 S. E. Shirsath, X. Liu, M. Assadi, A. Younis, Y. Yasukawa, S. K. Karan, J. Zhang, J. Kim, D. Wang and A. Morisako, *Nanoscale Horiz.*, 2019, **4**, 434–444.
74 X. Kou, S. Jiang, S.-J. Park and L.-Y. Meng, *Dalton Trans.*, 2020, **49**, 6915–6938.
75 Y. Lee, H. Lee, P. B. Messersmith and T. G. Park, *Macromol. Rapid Commun.*, 2010, **31**, 2109–2114.

76 C. Rocha, A. Latgé and L. Chico, *Phys. Rev. B: Condens. Matter Mater. Phys.*, 2005, **72**, 085419.
77 M. Kim, B.-H. Kwon, C. W. Joo, M. S. Cho, H. Jang, H. Cho, D. Y. Jeon, E. N. Cho and Y. S. Jung, *Nat. Commun.*, 2022, **13**, 1–9.
78 N. Amin and A. J. Peter, *Phys. B*, 2022, 413693.
79 Z. Li, C. Zhao, Q. Fu, J. Ye, L. Su, X. Ge, L. Chen, J. Song and H. Yang, *Small*, 2022, **18**, 2105160.
80 M. Li, J. Sun, G. Chen, S. Yao and B. Cong, *Appl. Catal., B*, 2022, **301**, 120792.
81 A. Saraiva, W. H. Lim, C. H. Yang, C. C. Escott, A. Laucht and A. S. Dzurak, *Adv. Funct. Mater.*, 2022, **32**, 2105488.
82 A. Rastelli, F. Ding, J. D. Plumhof, S. Kumar, R. Trotta, C. Deneke, A. Malachias, P. Atkinson, E. Zallo and T. Zander, *Phys. Status Solidi B*, 2012, **249**, 687–696.
83 A. Mittelstädt, A. Schliwa and P. Klenovský, *Light: Sci. Appl.*, 2022, **11**, 1–14.
84 X. Zhang, H. Xie, Z. Liu, C. Tan, Z. Luo, H. Li, J. Lin, L. Sun, W. Chen, Z. Xu, L. Xie, W. Huang and H. Zhang, *Angew. Chem., Int. Ed.*, 2015, **54**, 3653–3657.
85 Z. Sun, H. Xie, S. Tang, X. F. Yu, Z. Guo, J. Shao, H. Zhang, H. Huang, H. Wang and P. K. Chu, *Angew. Chem., Int. Ed.*, 2015, **54**, 11526–11530.
86 H. Gerischer, *Electrochim. Acta*, 1990, **35**, 1677–1699.
87 Y. Wang and A. Hu, *J. Mater. Chem. C*, 2014, **2**, 6921–6939.
88 H. Mattoussi, G. Palui and H. B. Na, *Adv. Drug Delivery Rev.*, 2012, **64**, 138–166.
89 C. Burda, X. Chen, R. Narayanan and M. A. El-Sayed, *Chem. Rev.*, 2005, **105**, 1025–1102.
90 A. Valizadeh, H. Mikaeili, M. Samiei, S. M. Farkhani, N. Zarghami, M. Kouhi, A. Akbarzadeh and S. Davaran, *Nanoscale Res. Lett.*, 2012, **7**, 480.
91 D. Bera, L. Qian, T.-K. Tseng and P. H. Holloway, *Materials*, 2010, **3**, 2260–2345.
92 K. Lasek, P. M. Coelho, K. Zberecki, Y. Xin, S. K. Kolekar, J. Li and M. Batzill, *ACS Nano*, 2020, **14**, 8473–8484.
93 A. Bouravleuv, V. Sapega, V. Nevedomskii, A. Khrebtov, Y. Samsonenko, G. Cirlin and V. Strocov, *J. Cryst. Grow.*, 2017, **468**, 680–682.
94 S. Thevuthasan, V. Shutthanandan, C. M. Wang, W. J. Weber, W. Jiang, A. Cavanagh, J. Lian and L. M. Wang, *J. Mater. Res.*, 2011, **19**, 1311–1314.
95 A. Ueda, D. O. Henderson, R. Mu, Y. S. Tung, C. Hall, J. G. Zhu, C. W. White and R. A. Zuhr, *MRS Proc.*, 2011, **396**, 441.
96 W. Chen, T. Shi, J. Du, Z. Zang, Z. Yao, M. Li, K. Sun, W. Hu, Y. Leng and X. Tang, *ACS Appl. Mater. Interfaces*, 2018, **10**, 43978–43986.
97 F. Palazon, Q. A. Akkerman, M. Prato and L. Manna, *ACS Nano*, 2016, **10**, 1224–1230.
98 S. Xin, P. Wang, A. Yin, C. Kim, M. Dobrowolska, J. Merz and J. Furdyna, *Appl. Phys. Lett.*, 1996, **69**, 3884–3886.
99 E. Kurtz, J. Shen, M. Schmidt, M. Grün, S. Hong, D. Litvinov, D. Gerthsen, T. Oka, T. Yao and C. Klingshirn, *Thin Solid Films*, 2000, **367**, 68–74.
100 K. Leonardi, H. Selke, H. Heinke, K. Ohkawa, D. Hommel, F. Gindele and U. Woggon, *J. Cryst. Grow.*, 1998, **184**, 259–263.
101 M. T. Swihart, *Curr. Opin. Colloid Interface Sci.*, 2003, **8**, 127–133.
102 A. Forleo, L. Francioso, S. Capone, P. Siciliano, P. Lommens and Z. Hens, *Sens. Actuators, B*, 2010, **146**, 111–115.
103 H. Zhang, J. Yu, C. Sun, W. Xu, J. Chen, H. Sun, C. Zong, Z. Liu, Y. Tang and D. Zhao, *J. Am. Chem. Soc.*, 2020, **142**, 16177–16181.
104 L. Hu, H. Zhong and Z. He, *Colloids Surf., B*, 2021, **200**, 111609.
105 Y. Liu, W. Zhang and W. Zheng, *Nano-Micro Lett.*, 2022, **14**, 158.
106 S. Mei, X. Wei, D. Yang, D. Su, W. Yang, G. Zhang, Z. Hu, B. Yang, H. Dai, F. Xie, W. Zhang and R. Guo, *J. Lumin.*, 2019, **212**, 264–270.
107 B. Mohanty, L. Giri and B. K. Jena, *Energy Fuels*, 2021, **35**, 14304–14324.
108 Y. Xu, L. Yan, X. Li and H. Xu, *Sci. Rep.*, 2019, **9**, 2931.
109 B. Shao, Z. Liu, G. Zeng, H. Wang, Q. Liang, Q. He, M. Cheng, C. Zhou, L. Jiang and B. Song, *J. Mater. Chem. A*, 2020, **8**, 7508–7535.
110 J. Zhang, C. Ling, W. Zang, X. Li, S. Huang, X. L. Li, D. Yan, Z. Kou, L. Liu and J. Wang, *Nanoscale*, 2020, **12**, 10964–10971.
111 H. Huang, Y. Xue, Y. Xie, Y. Yang, L. Yang, H. He, Q. Jiang and G. Ying, *Inorg. Chem. Front.*, 2022, **9**, 1171–1178.
112 Y. Liu, X. Li, Q. Zhang, W. Li, Y. Xie, H. Liu, L. Shang, Z. Liu, Z. Chen and L. Gu, *Angew. Chem., Int. Ed.*, 2020, **59**, 1718–1726.
113 G. Ou, P. Fan, X. Ke, Y. Xu, K. Huang, H. Wei, W. Yu, H. Zhang, M. Zhong and H. Wu, *Nano Res.*, 2018, **11**, 751–761.
114 X. Ren, L. Pang, Y. Zhang, X. Ren, H. Fan and S. F. Liu, *J. Mater. Chem. A*, 2015, **3**, 10693–10697.
115 L. Zhang, J. Xiao, H. Wang and M. Shao, *ACS Catal.*, 2017, **7**, 7855–7865.
116 F. Li, J. Li, Z. Cao, X. Lin, X. Li, Y. Fang, X. An, Y. Fu, J. Jin and R. Li, *J. Mater. Chem. A*, 2015, **3**, 21772–21778.
117 C. Zhang, Z. Pu, I. S. Amiinu, Y. Zhao, J. Zhu, Y. Tang and S. Mu, *Nanoscale*, 2018, **10**, 2902–2907.
118 Z. Pu, I. S. Amiinu, X. Liu, M. Wang and S. Mu, *Nanoscale*, 2016, **8**, 17256–17261.
119 S. Xu, D. Li and P. Wu, *Adv. Funct. Mater.*, 2015, **25**, 1127–1136.
120 X.-P. Yu, C. Yang, P. Song and J. Peng, *Tungsten*, 2020, **2**, 194–202.
121 W. Li, Y. Liu, M. Wu, X. Feng, S. A. Redfern, Y. Shang, X. Yong, T. Feng, K. Wu and Z. Liu, *Adv. Mater.*, 2018, **30**, 1800676.
122 Q. Dang, F. Liao, Y. Sun, S. Zhang, H. Huang, W. Shen, Z. Kang, Y. Shi and M. Shao, *Electrochim. Acta*, 2019, **299**, 828–834.
123 H. Cheng, M. L. Li, C. Y. Su, N. Li and Z. Q. Liu, *Adv. Funct. Mater.*, 2017, **27**, 1701833.
124 L. B. Huang, L. Zhao, Y. Zhang, Y. Y. Chen, Q. H. Zhang, H. Luo, X. Zhang, T. Tang, L. Gu and J. S. Hu, *Adv. Energy Mater.*, 2018, **8**, 1800734.

125 Y. Gong, L. Wang, H. Xiong, M. Shao, L. Xu, A. Xie, S. Zhuang, Y. Tang, X. Yang and Y. Chen, *J. Mater. Chem. A*, 2019, **7**, 13671–13678.
126 W. Zhang, X. Zhao, Y. Zhao, J. Zhang, X. Li, L. Fang and L. Li, *ACS Appl. Mater. Interfaces*, 2020, **12**, 10280–10290.
127 L. Huo, B. Liu, Z. Gao and J. Zhang, *J. Mater. Chem. A*, 2017, **5**, 18494–18501.
128 B. Ye, L. Huang, Y. Hou, R. Jiang, L. Sun, Z. Yu, B. Zhang, Y. Huang and Y. Zhang, *J. Mater. Chem. A*, 2019, **7**, 11379–11386.
129 S. Das, R. Ghosh, P. Routh, A. Shit, S. Mondal, A. Panja and A. K. Nandi, *ACS Appl. Nano Mater.*, 2018, **1**, 2306–2316.
130 Y. Liu, X. Zhang, W. Zhang, X. Ge, Y. Wang, X. Zou, X. Zhou and W. Zheng, *Energy Environ. Mater.*, 2022.
131 D. Dinda, M. E. Ahmed, S. Mandal, B. Mondal and S. K. Saha, *J. Mater. Chem. A*, 2016, **4**, 15486–15493.
132 F. Li, J. Li, Z. Cao, X. Lin, X. Li, Y. Fang, X. An, Y. Fu, J. Jin and R. Li, *J. Mater. Chem. A*, 2015, **3**, 21772–21778.
133 X. Ren, L. Pang, Y. Zhang, X. Ren, H. Fan and S. Liu, *J. Mater. Chem. A*, 2015, **3**, 10693–10697.
134 L. Najafi, S. Bellani, B. Martín-García, R. Oropesa-Nuñez, A. E. Del Rio Castillo, M. Prato, I. Moreels and F. Bonaccorso, *Chem. Mater.*, 2017, **29**, 5782–5786.
135 Z. Chen, H. Xu, Y. Ha, X. Li, M. Liu and R. Wu, *Appl. Catal., B*, 2019, **250**, 213–223.
136 T. Ali, X. Wang, K. Tang, Q. Li, S. Sajjad, S. Khan, S. A. Farooqi and C. Yan, *Electrochim. Acta*, 2019, **300**, 45–52.
137 Q. Zhou, X. Luo, Y. Li, Y. Nan, H. Deng, E. Ou and W. Xu, *Int. J. Hydrogen Energy*, 2020, **45**, 433–442.
138 C. Wang, M. Jin, D. Liu, F. Liang, C. Luo, P. Li, C. Cai, H. Bi, X. Wu and Z. Di, *J. Phys. D: Appl. Phys.*, 2021, **54**, 214006.
139 S.-Y. Pang, W.-F. Io and J. Hao, *Adv. Sci.*, 2021, **8**, 2102207.
140 L. Chen, J. Liang, Q. Zhang, X. Hu, W. Peng, Y. Li, F. Zhang and X. Fan, *Int. J. Hydrogen Energy*, 2022, **47**, 10583–10593.
141 S. Jeong, H. D. Mai, T. K. Nguyen, J.-S. Youn, K.-H. Nam, C.-M. Park and K.-J. Jeon, *Appl. Catal., B*, 2021, **293**, 120227.
142 S.-Y. Lu, S. Li, M. Jin, J. Gao and Y. Zhang, *Appl. Catal., B*, 2020, **267**, 118675.
143 Q. Shi and H. Liu, *Int. J. Hydrogen Energy*, 2021, **46**, 36763–36770.
144 J. Dong, X. Zhang, J. Huang, S. Gao, J. Mao, J. Cai, Z. Chen, S. Sathasivam, C. J. Carmalt and Y. Lai, *Electrochem. Commun.*, 2018, **93**, 152–157.
145 G. Zhao, P. Li, K. Rui, Y. Chen, S. X. Dou and W. Sun, *Chem. – Eur. J.*, 2018, **24**, 11158–11165.
146 S. Gao, B. Wang, X. Liu, Z. Guo, Z. Liu and Y. Wang, *Nanoscale*, 2018, **10**, 10288–10295.
147 Z. Pu, M. Wang, Z. Kou, I. S. Amiinu and S. Mu, *Chem. Commun.*, 2016, **52**, 12753–12756.
148 L. Lin, Z. Sun, M. Yuan, H. Yang, H. Li, C. Nan, H. Jiang, S. Ge and G. Sun, *ACS Sustainable Chem. Eng.*, 2019, **7**, 9637–9645.
149 W. Li, F. Li, X. Wang, Y. Tang, Y. Yang, W. Gao and R. Li, *Appl. Surf. Sci.*, 2017, **401**, 190–197.
150 I. W. P. Chen, C.-H. Hsiao, J.-Y. Huang, Y.-H. Peng and C.-Y. Chang, *ACS Appl. Mater. Interfaces*, 2019, **11**, 14159–14165.